CONF-9509230--10

TARGETS AND ION SOURCES FOR RIB GENERATION AT THE HOLIFIELD RADIOACTIVE ION BEAM FACILITY*

G. D. Alton
P. O. Box 2008
Oak Ridge, Tennessee 37831-6368

ABSTRACT

The Holifield Radioactive Ion Beam Facility (HRIBF), now under construction at the Oak Ridge National Laboratory, is based on the use of the well-known on-line isotope separator (ISOL) technique in which radioactive nuclei are produced by fusion type reactions in selectively chosen target materials by high-energy proton, deuteron, or He ion beams from the Oak Ridge Isochronous Cyclotron (ORIC). Among several major challenges posed by generating and accelerating adequate intensities of radioactive ion beams (RIBs), selection of the most appropriate target material for production of the species of interest is, perhaps, the most difficult. In this report, we briefly review present efforts to select target materials and to design composite target matrix/heat-sink systems that simultaneously incorporate the short diffusion lengths, high permeabilities, and controllable temperatures required to effect maximum diffusion release rates of the short-lived species that can be realized at the temperature limits of specific target materials. We also describe the performance characteristics for a selected number of target ion sources that will be employed for initial use at the HRIBF as well as prototype ion sources that show promise for future use for RIB applications.

*Research sponsored by the U.S. Department of Energy under contract No. DE-AC05-84OR21400 with Martin Marietta Energy Systems, Inc.

1. INTRODUCTION

Many of the reactions fundamentally important in nuclear physics, and astrophysics are inaccessible to experimental study using stable/stable beam/target combinations and therefore can only be studied with accelerated radioactive ion beams (RIBs). The availability of RIBs offers unique opportunities to further our knowledge about the structure of the nucleus, the stellar processes which power the universe and the nucleosynthesis burn cycles responsible for heavy element formation. As a consequence of world-wide interest in the potential benefits of using RIBs, facilities have been built, funded for construction or proposed for construction in Asia, Europe, and North America [1]; these include the Holifield Radioactive Ion Beam facility now under construction at the Oak Ridge National Laboratory (ORNL) [2].

The well-known on-line isotope separator (ISOL) technique can be directly applied in the generation of RIBs; the method is predicated on the production of radioactive nuclei in selectively chosen targets by proton, deuteron, helium, heavy ion, or neutron beams. The ISOL technique involves a multi-step process in which the reaction products are thermally diffused from the target, transported to the ionization chamber of an ion source, ionized, and separated according to mass in an on-line isotope separator (ISOL). The ISOL technique has been used to generate low energy RIBs from more than 68 of the elements in the periodic chart. For example, at the CERN-ISOLDE facility, approximately 600 radioactive beams representing 66 elements have been provided for research with intensities ranging up to 10^{12} ions/s [3]. For nuclear physics, nuclear structure physics, and astrophysics RIB research, the ion beam must be accelerated to the energy and intensity required for the particular experimental study. For these applications, beam intensities ranging from 10^5 to 10^{12} particles/s are typically required. The production rates in the target are set by practical limits on the

primary beam intensity in terms of the maximum permissible, on-target, power density which can be used without compromising the efficiency of the ion source or the physical integrity of the target, and the reaction cross sections for producing the species of interest. The radioactive product beam intensity is determined by the rate at which the particular species can be diffused from the target, the average residence time of the radioactive species on surfaces between the target and the ionization chamber of the source in relation to their lifetimes, the ionization efficiency of the ion source, and losses in beam transport between the ion source and experimental station. The upper temperature at which the target/ion source can be operated without deleteriously affecting the ionization efficiency is set by the vapor pressure characteristics of the target material [4, 5]. Because of these factors, careful attention must be given in the selection of the most appropriate target material, target design for the production and prompt and efficient release of the species of interest and in the design of an effective target/heat removal system that permits control of the target temperature during ion beam irradiation.

Equal care must be given in selecting the most appropriate ion source for a given species as well as in the mechanical design details of the specific source. The materials of construction of the target chamber, vapor transport tube and ionization chamber of the source can also significantly affect the residence times of the radioactive species through differences in magnitudes of the enthalpies of adsorption of the materials that the particle comes in contact with following diffusion release and transport to the ionization chamber of the source. A premium is placed on sources that can operate reliably for extended periods of time at elevated temperatures with good to excellent ionization efficiency.

In this report, we briefly review present efforts at the HRIBF to select the most appropriate target materials for generating RIBs, to design composite targets, to design effective target/matrix/heat removal systems that permit control of the target temperature during RIB generation with the objective of providing a means for effecting fast and efficient diffusion release of the radioactive ion beam of interest from the target material and fast effusive transport of the radioactive species to the ionization chamber of the source. We also describe a selected number of target/ion sources that will be employed for initial use at the HRIBF as well as prototype ion sources that show promise for future RIB applications.

2. PROCESSES WHICH AFFECT RELEASE TIMES

The principal means whereby short half-life radioactive species are lost between initial formation and utilization are associated with diffusion and surface adsorption processes where the release times are long with respect to the life-time of the species in question for forming RIBs. The diffusion and surface adsorption/desorption processes depend exponentially on the operational temperature of the target/ion source. Because of the strong temperature dependence of the adsorption process, the materials of construction of the target chamber, vapor transport tube and ionization chamber of the source can significantly affect the residence times of the radioactive species through the magnitudes of the enthalpies of adsorption on the surfaces of materials that the particle comes in contact with following diffusion release and transport to the ionization chamber of the source. The diffusion and surface adsorption processes are briefly described below.

2.1 Diffusion Theory

The time and temperature-dependent release of a nuclear reaction product species, embedded in a chemically dissimilar target material, implies the presence of a binary diffusion mechanism which underlies the release process. Whenever there is a concentration gradient of impurity atoms or vacancies in a solid material, the atoms or vacancies will move through the solid until equilibrium is reached [6]. The net flux, J, of either the atoms or the vacancies is related to the gradient of concentration, ∇n, by Fick's first equation given by:

$$J = -D\nabla n, \tag{1}$$

where D is the diffusion coefficient.

The time-dependent form of Eq. 1 is known as Fick's second equation. The three-dimensional form of this equation, which allows for the creation of particles S(x,y,z,t) as well as the loss of particles E(x,y,z,t), can be expressed in a Cartesian coordinate representation as follows:

$$\frac{\partial n}{\partial t} = D\left(\frac{\partial^2 n}{\partial x^2} + \frac{\partial^2 n}{\partial y^2} + \frac{\partial^2 n}{\partial z^2}\right) + S(x,y,z,t) - E(x,y,z,t) \tag{2}$$

where D is assumed to be independent of concentration.

The target geometries that will be used or are envisioned for use at the HRIBF include: planar, cylindrical and spherical geometries. For example, the time-dependent form of Eq. 2 appropriate for planar targets is given by

$$\frac{\partial n}{\partial t} = D\frac{\partial^2 n}{\partial x^2} + S(x,t) - E(x,t). \tag{3}$$

The equation, appropriate for diffusion from cylindrical geometry targets, where the diffusion process is assumed to move only in the r direction, can be expressed in the following form

$$\frac{\partial n}{\partial t} + \frac{D}{r}\frac{\partial}{\partial r}\left(r\frac{\partial n}{\partial r}\right) + S(r,t) - E(r,t). \tag{4}$$

While for spherical-geometry targets, where the diffusion process is assumed also to be solely in the radial direction, Fick's second equation takes the form:

$$\frac{\partial r}{\partial t} + \frac{D}{r^2}\frac{\partial}{\partial r}\left(r^2\frac{\partial n}{\partial r}\right) + S(r,t) - E(r,t). \tag{5}$$

Solutions to the respective time dependent forms of Equations 3, 4, and 5, appropriate for the particle target material geometry, can be found either by separation of variables, the use of Lapace or Fourier transformation techniques, or by standard numerical computational techniques or in combination.

We assume that the particles are either uniformly distributed during production of the radioactive species or in the case of ion implantation, the particles have a sharply Gaussian profile as represented below. For the more general case, the distribution function S must be chosen to represent the actual distribution of the radioactive species within the target material. For a uniform distribution of particles such as assumed in the production of radioactive species with a primary ion beam of intensity I and charge Z, S is given by

$$S(x,t) = \sigma N \ell I/Ze \tag{6}$$

where e is the charge on the electron, N the number of interaction nuclei per unit volume, ℓ is the length of the target material, and σ the cross section for production of the species of interest.

For the case where the distribution function S(x,t) is Gaussian, as would be the case for an ion implanted distribution, the function S is given by

$$S = \frac{I\sigma N\ell}{aeZ\sqrt{2\pi}} \exp\left[-\frac{1}{2}\{(x- < x >)/a\}^2\right] \tag{7}$$

where **a** is the standard deviation of the distribution and <**x**> is the depth of the distribution from the surface. For the ion implantation experiments, $\sigma N \ell = 1$. Where again I is the ion current of the primary beam of charge Z, e is the charge on the electron, **a** is the standard deviation of the distribution and <**x**> is the most probable depth of the distribution beneath the surface. For the case where the standard deviation of the distribution **a** is small, the particles are very localized beneath the target surface as is the case for ion implanted distribution. For stable element ion implantation, the E term is usually zero while for production of radioactive species with half-life $\tau_{1/2}$, is given by

$$E(x,t) = n\lambda \text{ where } \lambda = 0.693/\tau_{1/2}. \tag{8}$$

For solids, the diffusion process is dependent on the activation energy H_A required to move the atoms or vacancies from site to site is dependent upon H_A, and the temperature T according to:

$$D = D_0 \exp(-H_A/kT) \quad (9)$$

where D_0 is the intrinsic diffusion coefficient of the atom within the particular crystal matrix. D is related to the vibrational frequency and lattice parameters of the particular atom and crystal and k is Boltzmann's constant. H_A can be extricated from experimental data by measuring the dependence of D on target temperature T. As noted from Eq. 9, higher temperatures significantly affect release times of particles from the solid. Thus, in order to maximize the release of radioactive atoms from target material, it is desirable to operate the material to the limits set by the vapor pressure of the target material which do not compromise the ion source efficiency. The limiting vapor pressure of the sources presently used at the HRIBF is $\tilde{\leq} 2 \times 10^{-4}$ Torr [4].

2.2 Theory of Adsorption

Any time delays that are excessively long in relation to the life-time of the radioactive species can result in significant losses of beam intensity in an ISOL facility. The *residence time of a particle on a surface is given by the Frenkel equation:*

$$\tau = \tau_0 \exp[H_{ad}/kT], \quad (10)$$

where H_{ad} is the heat of adsorption or enthalpy required to evaporate the atom or molecule from the surface, k is Boltzmann's constant, T is the absolute temperature, and τ_0 is the time required for a single lattice vibration (~ 10^{-13} s). The heat of adsorption increases with increasing chemistry between the adsorbed atom and the surface where the adsorption takes place. This value varies widely depending upon the adsorbent/adsorbate combination.

The desorption rate of adsorbed atoms per unit area dn/dt in thermal equilibrium with a surface at temperature T is given by

$$\frac{dN}{dt} = S(T)N\frac{\omega_0}{2\pi}\exp[-H_{ad}/kT] \qquad (11)$$

where S(T) is the temperature-dependent probability that the particle will stick to the surface (sticking coefficient), N is the number of atoms adsorbed per unit area, and $\omega_0/2\pi = 1/\tau_0$.

Since it is desired to minimize the residence times of atoms/molecules on surfaces in the target/ion source, the choice of the materials of construction for the vapor transport system of the source is extremely important. Coating the inner surfaces of the vapor transport tube (usually made of Ta or W) with a chemically inert material is expected to significantly reduce residence times and, therefore, the noble metals, iridium- or rhenium, have been recommended for this use [7, 8].

3. TARGET SELECTION

The most difficult challenge related to the efficient generation of RIBs using the ISOL technique is associated with target issues and not the ion source itself. The requirement of fast diffusion from the target not only involves the physical, chemical, and metallurgical properties of the target material/RIB species combination, but also the target particle size and geometry, as well. The short-lived radioactive species must escape from the interior of the target material by classical diffusion processes which are strongly dependent on the physio-chemical properties of the species of interest in relation to those of the target material (activation energy) and the temperature of the

target. The speed of release is dependent on the diffusion constant, the target temperature and the length of the target material through which the particle must pass prior to arriving at the surface of the target material. Therefore, fast release times are synonymous with large diffusion constants, short diffusion lengths (i.e., small target dimensions), low enthalpies for adsorption and as high as practicable, target temperatures. Upon arrival at the surface of the target material through diffusion, the atom of interest must be evaporated from the target material and effused into the ionization chamber of the ISOL source without significant time delays. Therefore, the adsorption times (sticking times) due to chemical reactions between the radioactive species and the materials from which the source are made must be minimized.

The selection of production targets that will swiftly, efficiently and selectively release minute quantities of the short lived species in the presence of bulk quantities of the target material itself is difficult because of the lack of an extensive list of refractory target materials from which to choose that also have the fast diffusion release properties required of the element of interest. A solution to this challenging problem can be reached only by careful consideration of the physical, chemical, and metallurgical properties of the radioactive species in relation to those of the target material and by careful and thoughtful design of highly permeable target matrix systems with short diffusion lengths and controllable target temperatures. The challenge is to select a target material which will withstand the high temperatures required to efficiently, and promptly release the short lived species of interest while preserving the vacuum requirements of the ion source [4, 5]. Ideally, the target should be a finely divided powder which does not sinter, melt or vaporize excessively at the operating temperature of the target/ion source; or thin disks; or small diameter cylinders. The particles, disks or cylinders should be spaced apart in a highly permeable arrangement so that diffusion lengths of the species within the target

material are short and the delay times due to effusive processes are minimized.

3.1 Target Material Considerations for the HRIBF

Target material selection begins by considering the physical, chemical, and thermodynamic properties of the target material in relation to those of the product species. The primary problem lies in the availability and proper choice of target materials which are sufficiently refractory so that they can be heated to the elevated temperatures necessary for fast release of the product radioactive species without vaporization or sublimation of the target material itself. The maximum target temperature is limited by the vapor pressure of the target material which must be kept sufficiently low so as to avoid spoiling the rather stringent vacuum levels required for efficient ionization [4, 5]. The choice of target material is further restricted by the requirement that the radioactive species must be easily diffused from the target and readily volatilized for subsequent ionization. This requires that the species itself not be refractory and that it not form refractory compounds within the target material. The radioactive species should, in the ideal case, possess physical and chemical properties almost opposite to those of the target; that is, they should be easily diffused from the target material either in elemental or in compound form and upon exit, be readily desorbed from the target surface. Furthermore, this difference in the physical and chemical properties between the target material and the radioactive species must exist for elements which lie within a few atomic numbers of each other because of the low-mass projectiles from ORIC for the fusion reactions required to produce proton-rich nuclei. These idealized differences in chemical and physical properties which are desirable for fast release of the species of interest are not often practically realizable, particularly for close-lying elements where their physical and chemical properties are often similar. Obviously, compounds are desirable which contain the highest

percentage of the element of interest so as to maximize the production rate of the desired RIB. Still other factors which complicate the choice of target material, such as the production of unwanted, long-lived radioactive by-products, must also be taken into consideration.

Tables IA and IB provide a partial listing of candidate target materials that have been selected for potential use at the HRIBF; these materials were selected because of their low vapor pressure characteristics in relation to those of the radioactive species that must be diffused from the target material. Only a few of the targets have been evaluated in off-line experiments and by the ion implantation method (see, for example, Refs. 7 and 8). None have been used, to date, for generation of RIBs at the HRIBF. Each of the target materials will be evaluated by use of ion implantation of stable complements of the RIB species of interest before arriving at a definitive answer of their suitability for RIB generation. As classic examples of the ideal target/radioactive species combination, we cite cases such as the production of ^{13}N in C to form the gaseous species CN_2 or for the generation of ^{14}O and ^{15}O in a C target to form the noble molecule CO or in the generation of ^{30}S in SiO_2 to form the SO_2 molecule where the release product again is gaseous. Not all release products are gaseous and for these cases, the selection is based on the volatility of the product compound in relation to the target material itself. These systems are obviously more complicated and less likely to be successful because of the prospects of long diffusion delay times (larger activation energies) in relation to the life-time of the radioactive species during release from the target material. Figure 1 illustrates how the first step in the target selection process is made when only vapor pressures are known about the target material/radioactive species couple. For example, the vapor pressures of Al_2O_3 and AlF_3 are shown in Fig. 1; Al_2O_3 is a candidate target material for use in generating ^{17}F and ^{18}F; the fluorine will, more than likely, be released in the molecular form AlFx.

The volatility of partially fluorinated AlFx compounds are unknown; however, if by chance there is sufficient F available for satisfying the valence of Al, then the product molecule would be very volatile, as illustrated. Following preliminary selection of the target material by this method, the target material is subjected to a more definitive test by measuring the release times for diffusion of the species of interest from the target material by use of the ion implantation technique, described below. In general, each element must be considered separately, often requiring dedicated efforts to solve specific problems, in order to generate useful RIBs of the element of interest. Much work remains to be done in the area of target material selection and the development of techniques to enhance the release of elements from a properly chosen target material.

3.2 Ion Implantation Release Studies

Ion implantation offers a cost effective and powerful technique for predetermining the time-release behavior of stable complements of interesting radioactive species from target materials which are candidates for their generation, as well as a straightforward method for determining diffusion coefficients for many element/target combinations. This technique is being used at the HRIBF to select the most appropriate target material for generating a particular radioactive ion beam (RIB) (see, for example, Refs. 7 and 8). In these experiments, the 25-MV HRIBF tandem accelerator is used to implant stable complements of interesting radioactive elements into refractory targets mounted in a high-temperature version of the FEBIAD ion source [9] which is on-line at the UNISOR facility [10]. The operational temperature of the version of the FEBIAD ion source used in the ion implantation release studies is approximately 1645°C and cannot be varied. The inability to vary the target temperature prevents taking advantage of the exponential behavior of the diffusion process with temperatures and

evaluation of targets that could, otherwise, be operated at higher temperatures or prevents evaluation of target materials that must be operated at lower temperatures.

The target material is mounted in the anode structure of the FEBIAD ion source; energetic heavy ion beams from the 25 MV tandem accelerator pass through a thin window of some heavy elemental material, such as tantalum which acts to seal the target chamber to prevent particle loss following diffusion release from the target. The final energy after passing through the window is chosen so that the ions penetrate to a depth of ~ 2 to 35 μm in a thin circular disk of the target material being evaluated. (The target material is usually very thick compared to the implantation depth, thus can be considered semi-infinite when solving the appropriate form of the diffusion equation (Eq. 3, for example). Upon deposition within the target, the neutral species diffuse randomly in the high-temperature sample, which is maintained at a temperature of ~1645°C prior to implantation. Beam heating effects raise the target temperature in proportion to the beam power; this effect has been measured; typically a 10-Watt beam raises the temperature by an additional 50°C. Thus the target resides at ~1700°C during the implantation. Particles which diffuse out of the face of the beam entry side of the target are evaporated from the target surface and are transported into the anode region of the ion source through effusive flow. After passing into the anode structure, they are bombarded with an electron beam accelerated from a hot cathode. A fraction of the particles are ionized, extracted from the ion source, mass analyzed, and the signal versus time of the mass selected species is recorded with the "beam-on-target"; the signal rises according to the release rate of the implanted species and reaches saturation or a constant value, at which time the beam is removed from the target. During the "beam-off-target" time period, the intensity decreases with time and is monitored until the signal reaches background levels. The time required for releasing 50% of the saturation level is defined as the release time for the particular species

from the target material.

The simulation program, TRIM, which calculates the energy loss of the projectile while slowing down in the target material, is used to numerically determine the position <**x**> and distribution of the implanted species within the target material [11]. The depth <**x**> and distribution of the implanted material depends on the projectile, the projectile energy, and atomic number of the constituents which make up the target material, as well as the density of the target material. Figure 2 displays the distribution function for an energetic heavy ion beam implanted into a target material. This distribution is used to derive the parameters for the creation function S defined in Eq. 7. A simulation program, called DIFFUSE [12] is used to solve Fick's second equation (Eq. 3) and determine the diffusion coefficient D for the particular species/target material combination. The input parameters, required by DIFFUSE to fit to the experimental data include the particle distribution function as calculated by the use of TRIM and the diffusion coefficient D.

Release times and diffusion coefficients. Diffusion coefficients are of crucial importance toward the understanding of the diffusion release process and for predictions of the release times of the species in either of the previously described target geometries and at other temperatures. Exact diffusion coefficients D can be derived by fitting solutions to either Equation 3, 4, and 5, depending on the target geometry, to experimental release data or be estimated from ion implantation release experiments. For the latter case, the diffusion coefficient D_e can also be estimated by using the following simple relationship:

$$D_e \simeq C_o \langle \mathbf{x} \rangle^2 / \tau \qquad (12)$$

where <**x**> is the most probable depth of implantation and τ is the release time at the 50% point, and C_0 is a constant. For the ion implantation data, C_0 is found to be ~ 1. This greatly simplifies the determination of D by providing starting values for fits to the experimental data. The diffusion coefficients can then be used to predict release times of short-lived radioactive complements of the stable implanted species from homogeneously distributed, planar-, cylindrical- or spherical-geometry samples at the same temperature which are the principal target geometries that will be used for actual RIB generation.

Figure 3 compares the experimentally measured time-release profiles of ^{37}Cl implanted to a depth of 2.6 μm in CeS (target temperature: 1690°C) with fits to the data derived by use of DIFFUSE [12]. The dashed line, superposed on the experimental data, represents a computational fit for a Gaussian distribution for S, as given by Eq. 7. As noted, the fits to the release profile are exceptionally good.

During operation of the HRIBF, the radioactive species will be uniformly distributed within either planar, cylindrical or spherical targets. The time-release information derived from ion implanted targets, which have sharply Gaussian distributions, is only of qualitative value for estimating release of radioactive species from RIB target materials where the nuclear reaction products are more or less uniformly distributed within the sample. Since release times are dependent on the initial distribution, as well as the depth of the implanted material, information derived from implantation experiments cannot be directly used to predict release times of the complementary, short-lived, homogeneously distributed, radioactive species. However, the diffusion coefficients, extricated from ion implantation experiments, can be used to predict release times of the particular species from the same target material, in different geometries and at other temperatures. In order to use solutions to Fick's equation

(Eqs. 3, 4, and 5) for making predictions at temperatures other than those used in the ion implantation experiments, the activation energy must be known. As an example of such predictions, Fig. 4 displays theoretical "beam-on-target" and "beam-off-target" time-release spectra for ^{37}Cl and ^{33}Cl diffusing from homogeneously distributed, 5-μm-diameter spherical-geometry macro-particles of CeS at 1690°C and 1990°C. The predictions made for the diffusion release at a target temperature of 1990°C were estimated by assuming an activation energy of 1.0 eV. This value may be too low, but is reasonable in relation to measured values commonly found in the literature (see, e.g., Ref. 6).which correlates with an intrinsic diffusion coefficient, $D_o = 1.6 \times 10^{-7}$ cm^2/s. The diffusion coefficient D at the temperature for which the release measurements were made is $D = 4.4 \times 10^{-10}$ cm^2/s.

The time-release behavior of 209 MeV Se ion beam implanted into and released from a Zr_5Ge_3 target is displayed in Fig. 5. The solid line is a fit to the data derived by solution of Eq. 3 with S defined by Eq. 7 for a Gaussian distribution function with DIFFUSE. More details concerning the experimental methods utilized and the time release behavior for other projectile/target material combinations are given in Refs. 7 and 8. The theoretically predicted release of ^{78}Se and ^{71}Se homogeneously distributed from planar and macro-spherical geometry spherical targets are shown in Fig. 6. The release profiles for the 20-μm-thickness planar-disk targets which are, in fact, too thin to fabricate in practice, serve only as a means of comparison of the planar disk targets with the practically sized, 20-μm spherical-geometry targets. It is obvious that spherical macro-particle target materials are always desirable if one can avoid sintering the materials during the release process. The actual release times for radioactive particles which have been released by diffusion from spherical particles will be moderated by the hold-up times associated with the times required to migrate through the distribution of material. These times may be long enough to offset any

advantage gained by using spherical particles coupled with the fact that the target must be operated at temperatures below the sintering temperature (~ 80% of the melting point of the particular material).

Table II provides a condensed summary of the release times and diffusion constants derived from previous implantation studies; not all of the data listed have any relevance for choosing target materials, rather, some of these data were collected to determine the release properties of candidate materials for removal of heat from the target when intermixed with the target material for production of the RIB species. For example, the release data for Ga and Cu from C and BN were collected to assess the merits of these material as agents for heat removal from particulate ZnO for the production of ^{64}Ga and from particulate NiO for the production of ^{58}Cu. Many of the diffusion coefficients D_e were estimated solely by use of Eq. 12. As noted, there is good agreement between the values predicted from Eq. 12 with those extricated by fits to the experimental data. The experimentally measured release profiles reflect the total accumulated time required for diffusion τ_d, effusion τ_e, and ion transport τ_s to the detector system following mass analysis. The diffusion coefficients and release times derived from the data are only valid whenever $\tau_d >> \tau_e + \tau_s$ or whenever τ_e and τ_s are known. While τ_s is always precisely known, τ_e must be estimated or measured independently. This criterion is met for species/target combinations described in this paper.

The results of ion implantation studies clearly demonstrate that the technique can be utilized as a practical and cost-effective means for evaluating candidate refractory targets for releasing specific elemental materials prior to their actual use in generating radioactive ion beams. Diffusion coefficient information derived from such experiments can be used to realistically estimate beam intensities which could be

produced in a particular ISOL ion source during RIB generation. Diffusion coefficients extracted from this data can also be used to optimize the target particle size and geometry in order to minimize the release time of the element of interest from the candidate target material. In addition, important information can be learned about the character of the target material regarding the upper temperature limit at which a particular target can be operated to avoid excessive sublimation and vaporization of the target, thereby spoiling the source efficiency. The quality of the target material in terms of the presence, or lack thereof, of isobaric contaminants which could cause problems during actual RIB generation and acceleration can also be evaluated.

4.0 NEW CONCEPT TARGET DESIGNS

New target concepts are presently under development at the HRIBF that, in principle, can be applied in the design and fabrication of targets with short diffusion lengths and high permeability properties required if present RIB facilities are to be successful in meeting the intensity and species needs of their respective research programs. These new technologies include the choice of low-density target matrixes, such as carbon-bonded-carbon fiber (CBCF) or reticulated carbon (RC), which can be used as the thermal transport structure for the removal of heat from the target material and as the plating matrix for the target material itself. Since short-lived particles must swiftly diffuse from the target material, the diffusion lengths must be short (thin target materials), and the target temperature must be as high as practicable. Techniques are presently available that can be used to uniformly deposit specified thicknesses of the material in question onto the support matrix of choice. At this point in time, several target coating schemes are being used or are under consideration for this purpose, they include: 1) chemical vapor deposition (CVD); 2) plasma vapor deposition (PVD);

and 3) sol-gel coating. In addition, cataphoretic or electrophoretic coating techniques are also under consideration as viable means for coating target matrix support structures with specified thicknesses of material.

4.1 The Composite Target Matrix System

The objective of the development program is to develop thin but highly permeable target matrix/heat-sink systems that, in combination, will permit operation of the target matrix at the maximum temperature allowable during production of radioactive species. The projectiles that will be utilized to produce the radioactive species at the HRIBF will be ^{1}H, ^{2}H, ^{3}He or ^{4}He projectiles at energies between 10 and 70 MeV and ion beam intensities up to 50 μA. The maximum beam power that can be utilized while generating a particular RIB will be dictated by the maximum target temperature to which the composite target matrix can be operated without compromising the ion source efficiency which is governed by the vapor pressure in the source [4, 5]. During passage through the target material, the beam will deposit significant amounts of energy in the target primarily through electron-electron and nuclear-nuclear interactions with the atoms which comprise the target material. More-over, the target system is also heated to approximately 750°C by conduction along the vapor transport tube to the target housing from the cathode of the source which operates at ~ 2025°C. The target system is provided with an external heater system which surrounds the target so that heat can be added when required. The total energy must be carefully balanced during production by providing an effective heat-sink system that is designed to remove the heat from the target material at a controlled rate so as to maintain a specific temperature which is set by the vapor pressure of the target material.

Figure 7 schematically represents three composite target schemes, among other target

systems under consideration for possible use in fabricating targets at the HRIBF. The target scheme includes macro-particles, 5-10 μm in diameter, coated or uncoated with Re; as thin as practicable disks which may be fabricated from the material of interest or be composites of, e.g., Re coated C with ~ 10 μm of the material of interest on both sides. (The disks will be mounted in the target/heat-sink system with spacing between the them to ensure fast release); or a composite target system composed of thin fiber diameter or CBCF onto which is coated ~ 10 μm of Re followed by a thin layer (~ 5-10 μm) of the material of interest. The choice of the particular target matrix system will depend on the availability of techniques for uniformly coating the target material onto the composite target matrix at the thicknesses required for efficient and fast diffusion release and the results of thermal transport studies. Figure 8 displays SiC which has been CVD deposited on CBCF (fiber diameter ~ 6μm) as considered for the generation of ^{30}S. The CBCF is precoated with ~ 1μm of Re prior to CVD coating of the SiC. As noted, the target matrix is highly permeable and therefore the release efficiency should be high.

4.2 The Prototype Composite Target/Heat-Sink System

The efficiency of the ionization process is strongly dependent on the pressure in the ionization chamber of the source and thus the vapor pressure of the target material; the vapor pressure of the target material is, in turn, strongly dependent on the target temperature; therefore, control and maintenance of a specific temperature, below a critical value, in the target holder/target matrix region of target/heat sink assembly is critically important for successful and efficient generation of high intensity RIBs. To achieve the primary objective of the project, the target/heat-sink assembly design will be optimized so that the particular target composite matrix can be maintained at a prescribed temperature which is limited by the maximum vapor pressure of the target

material that can be tolerated before compromising the ion source efficiency and/or destroying the target through sublimation/vaporization processes.

Our objectives are to optimally design a target/heat-sink assembly similar to that shown in Fig. 9 using the finite element computer code ANSYS [13], so that the temperature of the target matrix can be maintained and controlled at a prescribed value when irradiated with protons, deuterons, ^{3}He and ^{4}He of sufficient energy per particle to optimize the production of the radioactive species of interest. In order to design the target/heat-sink assembly, the computer code is used to simulate the transport of heat generated by high energy ion beams as they interact with the target material. The finite element heat transfer code FLOTRAN [14] will be used to supply the heat transfer coefficients between the heat sink boundary and the water heat exchange medium. The effects of thermal expansion, the dependence of thermal conductivity and emissivity on target temperature are included in the ANSYS calculations. It is necessary to supply the code with certain physical properties (thermal conductivities, emissivities, etc.) of the materials from which the various components of the target holder/heat-sink assembly are made; these properties include those of the target holder, the target matrix materials, those of the beam stop, the heat deposited in the target and beam stop by the beam per unit path length as it traverses the target and comes to rest within the beam stop as well as those of the heat exchange medium and heat exchange interface. This information will, in general change for each projectile/projectile energy/composite target-matrix combination considered. Certain material properties which are not available from the literature such as thermal conductivities for composite materials with less than theoretical density, special alloys, or ceramics, etc. will be measured. The energy loss (stopping power) function is calculated by the use of the computer code TRIM [11]. This data is used as input into ANSYS. As a matter of policy, the target thickness where the

particle energy loss becomes very large is always chosen so that high energy density region of the dE/dx curve occurs in the beam stop to avoid excessive heating of the target material itself. This region corresponds to the Bragg peak where the projectile energy is below the coulomb barrier and, therefore, is ineffectual for producing nuclear reactions.

A prototype composite target/heat-sink system now under design at the HRIBF is displayed in Fig. 9. The device can be inserted into or removed from the target/ion source through a vacuum inter-lock port. The primary beam enters the target after passing through a thin window of Re and a highly permeable Re coated CBCF thimble which contains the composite target matrix. The primary projectile beam, which produces the radioactive species, will be slowed down in the composite target material where it deposits energy and finally comes to rest in a beam stop of either C or Be. The energy deposited in the composite matrix will raise it to a certain temperature; the maximum, steady state temperature of the composite target matrix will depend on the physical, chemical and thermodynamic properties of the materials which make up the assembly and those of the heat exchange medium used to remove heat through conduction at the beam-stop/heat-exchange interface. The energy loss per unit length dE/dx (stopping power) of the target matrix material will depend on the type and energy of the primary projectile ion beam, materials of construction and design details of the assembly.

5. SELECTION OF ION SOURCES FOR INITIAL USE AT THE HRIBF

The ISOL technique is complicated by high-temperature physics, chemistry, metallurgy, diffusion, and surface adsorption processes which take place in the target/ion source; all of these processes add to the delay times which result in losses

of the short-lived radioactive species of interest. The target ion source program is aggressively designing and developing target/ion sources for the future HRIBF research program [15, 16]. The selection and design of the ISOL/target ion source system is of critical importance since its performance determines the efficiency of ionization, the intensity, and number of RIBs that can produced for experimental use. Since the HRIBF will use the 25-MV tandem accelerator for the acceleration of RIBs to energies appropriate for research in nuclear physics, negative ion beams are, therefore, required for injection into the tandem accelerator. Because charge exchange is an efficient means for converting initially positive ion beams into negative ion beams, both positive and negative ion beams are viable options for use at the facility. Careful consideration must also be given in selecting the most appropriate ion source for efficiently ionizing the species delivered to the ionization chamber of the source. For RIB generation, the source should ideally exhibit the following properties: high efficiency; high temperature operation in order to minimize the diffusion times from the target and short residence times on the surface; low energy spreads; chemical selectivity; flexibility for adaptation to different temperature ranges and modes of operation; target temperature control; long lifetime; and stable electrical and mechanical properties. The source should, as well, be designed for safe and expedient insertion/removal from the ISOL facility to permit changing of the target material and for source repairs.

A number of ion sources have been designed and evaluated for potential use in the HRIBF research program. A modified form of the high-temperature CERN-ISOLDE-type positive-ion source [17] has been designed for initial use at the HRIBF [15, 16]; referred to as the EBPIS. In addition to the EBPIS, a Penning Ionization Gauge (PIG) source has been designed and evaluated, and a combined thermal dissociation and electron impact ionization source has been conceived which, in principle, will

overcome the handicap of the spectrum of molecular beams emitted by more conventional electron impact ion sources. A dual-purpose, positive or negative surface ionization source also has been designed for generating ion beams from the more electro-positive and electro-negative members of the periodic chart. Future plans call for the design and development of new concept ECR ion source specifically tailored for RIB generation. HRIBF target/ion source development program is aggressively developing rf, positive ion sources and plasma-sputter, cesium sputter, negative ion sources for generating particular RIB species.

5.1 The Electron Beam Plasma and Penning Ionization Source

ISOL ion source development continues to be driven by needs for sources with improved chemical selectivity, high duty factors, and more universal species capabilities. Despite the fact that electron beam plasma ion sources have poor chemical selectivity characteristics, they have a decided advantage in that they are closer to being universal than other ISOL sources that have been developed to date. A modified form of the high-temperature version of the CERN-ISOLDE source has been selected as the first source to be used for the generation of RIBs at the HRIBF. a number of reasons, including the following: 1) it is competitively efficient; 2) it has demonstrated reliability over many years of operation at CERN-ISOLDE; 3) the target temperature can be controlled independently of the discharge parameters of the source; 4) it can be readily adapted for a wide range of operational temperatures and for other modes of operation; 5) it is readily adaptable to other types of ion sources; 6) it has been engineered for safe removal and installation in the high level radiation fields incumbent at an ISOL facility; it has a low-emittance and a wide range of species capability.

A cross-sectional side view of the target/ion source assembly, mounted on the voltage platform of the HRIBF, is shown in Fig. 10. The side and top views of the high-temperature EBPIS are shown schematically in Figs. 11 and 12. A Penning Ionization Gauge version of the source has also been designed and evaluated. The source, shown in Fig. 13, is a simple modification of the EBPIS. These sources are presently in the second iteration of development in an effort to improve their ionization efficiencies overcome certain problems endemic with the original source design.

RIB production is accomplished by irradiation of the chosen target material with beam of protons, deuterons ^{3}He or ^{4}He particles. During the irradiation, a collimated ion beam from the ORIC will pass through a thin Re window where it interacts with the refractory target material chosen for the production of the desired radioactive beam. The Ta target material reservoir is lined with Re metal as is the beam transport tube and all internal surfaces that particles come in contact following diffusion release from the target material. Collimation of the electron beam is effected by adjusting the coaxially directed solenoidal magnetic field so as to optimize the ionization efficiency of the species of interest. The cathode power required to achieve thermionic emission temperature is ~ 1.2 kW. The total power required to heat the ISOL/target and cathode to the temperatures listed above and to ionize the vaporous material transported from the target to the ionization chamber of the source will be of the order of 3.5 kW. Ionization efficiencies for Xe from both sources are typically ~ 15-20%. The emittances of the two sources are comparable. Figure 14 displays emittance contours for the EBPIS while the complementary contours for the PIGIS are shown in Fig. 15; the normalized emittances versus percentage of ion beam for the two sources are compared in Fig. 16.

5.2 Estimates of the Ionization Efficiencies for Electron Beam Plasma Ion Sources

ISOL sources are routinely equipped with standard leaks of a noble gas, usually Xe, which is continually fed into the source at a known feed rate to enable real-time determination of the source performance. This information is then used as a gauge for determining the relative ionization efficiency for the species of interest. Since the ionization potentials for the noble gases range from 24.46 eV (He) to 10.7 eV (Rn), the efficiencies at which a particular source can ionize each of these elements can serve as a valuable figure of merit for a particular source type. Electron impact ionization sources of the FEBIAD-CERN-ISOLDE type like the EBPIS are quite efficient for low-ionization-potential elements and elements which are heavy and, therefore, move slowly through the ionization volume of the source. However, those sources do not ionize low-mass elements, especially those with high ionization potentials. The measured ionization efficiencies for the noble gas elements, as reported in Ref. 18, are, respectively, Ne: 1.5%; Ar: 18%; Kr: 36%; and Xe: 54%. The following equation is found to be useful in approximating the ionization efficiencies η for the noble gases:

$$\eta_{calc} = \frac{4 < \ell > D_o N_e}{A_o} \left(\frac{\pi Mi}{8kTi}\right)^{1/2} \exp\left\{-I_p / < kT_e >\right\} /$$

$$\left[1 + \frac{4 < \ell > D_o N_e}{A_o} \left(\frac{\pi M_i}{8kT_i}\right)^{1/2} \exp\left\{-I_p / < kT_e >\right\}\right] \qquad (13)$$

where $< \ell >$ = average path length for a particle in the plasma; D_o is a constant (cm^2/s); A_o is the emission area of the source; k is Boltzmann's constant; T_i is ion temperature; T_e is the electron temperature; I_p is the ionization potential; N_e is the number of electrons in the valence shell of the atom with a given I_p; and M_i is the mass of species.

The following values are used for terms in Eq. 13 when estimating ionization efficiencies for the FEBIAD ion source: $< kT_e > = 3$ eV; $T_i = 2273°K$; and $4<\ell>D_o/A_o = 5.39 \times 10^3$ cm/s. Table III compares measured ionization efficiencies [Refs. 18-20] with those calculated by use of Eq. 13.

5.3 Ion Sources for Future Use at the HRIBF

A New Concept Thermal Dissociator/Electron Impact Ion Source. Many chemically active radioactive species are released from the target material in molecular form. Because of the low probability of simultaneously dissociating and efficiently ionizing the individual molecular constituents with conventional, hot-cathode, electron-impact ion sources, the ion beams extracted from these sources often appear as a mixture of several molecular sideband beams. Because of the low probability of both dissociating the molecule and efficiently ionizing the constituents of the molecule in the EBPIS, ion beams of these species are partitioned in several mass channels. In this way, the intensity of the species of interest is diluted. We have designed an ion source that combines the excellent molecular dissociation properties of a thermal dissociator and the high efficiency characteristics of an electron impact ionization source. Because beam intensity for RIB applications is at a premium, it is quintessential to have as much of the RIB species, as practicable, in a single mass channel so that the beam intensity is a high as possible. The source is described in these proceedings [21].

The Positive/Negative Surface Ionization Source. A versatile, spherical-geometry, positive/negative surface ionization source has been designed and fabricated and awaits evaluation for generation of both positive and negative ion beams for potential use at the HRIBF. The utility of the new positive/negative surface ionization source

concept is that the ionizer can serve both as a negative or positive surface ionizer by simply using or not using cesium. The source is designed to be a complementary replacement for the high temperature, EBPIS. The vapor transport tube will be Re coated tantalum and heated resistively to ~ 1100°C. The ionizers are made of either highly permeable CBCF or RC composite matrixes coated with ~ 10 μm of Ir. These mesh-type surface ionizers will be more effective in ionizing vapor than ionizers predicated on the reflection of vapor onto a solid surface, since particles must pass through the highly permeable Ir mesh before exiting from the source. Since Ir has a very high work function (~ 5.29 eV), the source is quite efficient for highly electropositive elements such as members of the group IA and group IIA elements, for example. The ionizer can also be used to produce negative ion beams from highly electronegative species without any mechanical changes. For negative ion formation, cesium or another volatile highly electropositive element from an external oven is fed through the high permeability ionizer matrix at a rate commensurate for maintaining approximately 0.5 monolayer of the adsorbate on the surface which lowers the work function to ~ 1.43 eV for Cs and ~ 2.13 eV if, for example, Ba were chosen for use. The source is described separately in these proceedings [22].

New Concept ECR Ion Sources for RIB Generation. Future plans call for the use of an all permanent magnet ECR source with a tailored central magnetic field designed to create a large resonant plasma "volume." The magnetic field will be designed to optimize low charge rate RIBs as required for charge exchange generation of negative ion beams. The new "volume" type source will be a derivative of the source concept described in Refs. 23 and 24 and the new concepts ECR source described in these proceedings [25].

Acknowledgments

The author is indebted to H. K. Carter, J. Breitenbach, S. Ichikawa, and J. Kormicki of the UNISOR group for assistance during the ion implantation experiments and to J. Dellwo for assistance in analyzing the data.

References

[1] D. K. Olsen, Nucl. Instr. and Meth. A328, 303 (1993).

[2] A Proposal for Physics with Exotic Beams at the Holifield Heavy Ion Research Facility, eds. J. D. Garrett and D. K. Olsen, Physics Division, ORNL, March 1991, unpublished.

[3] H. L. Ravn in ISOLDE User's Guide, Ed. H. -J. Kluge, CERN 86-05 (1986).

[4] R. Kirchner and E. Roeckl, Nucl. Instr. and Meth. 133, 187 (1976).

[5] P. Van Duppen, P. Decrock, M. Huyse, and R. Kirchner, Rev. Sci. Instr. 63, 2381 (1992).

[6] See, for example, *Diffusion in the Condensed State*, J. S. Kirkaldy and D. J. Young (The Institute of Metals, London, 1987), Ch. 1.

[7] G. D. Alton, H. K. Carter, I. Y. Lee, C. M. Jones, J. Kormicki, and D. K. Olsen, Nucl. Instr. and Meth. B66, 492 (1992).

[8] G. D. Alton, J. Dellwo, H. K. Carter, J. Kormicki, G. di Bartolo, J. C. Batchelder, J. Breitenbach, J. A. Chediak, K. Jentoff-Nilsen, and S. Ichikawa, Proc. of the International Conference on Neutrons and their Applications, eds. G. Vourvopoulos and T. Paradellis, SPIE, Vol. 2329, p. 335.

[9] R. Kirchner, D. Marx, O Klepper, V. T. Koslowsky, T. Kühl, P. O. Larsson, E. Roeckl, K. Rykaczewski, D. Schandt, J. Eberz, G. Huber, H. Loehmann, R. Menges, and G. Ulm, Nucl. Instr. and Meth. A234, 224 (1985).

[10] UNISOR, Oak Ridge Associated Universities, Oak Ridge, TN 37831, USA.

[11] TRIM - The Transport of Ions in Matter, J. F. Ziegler, IBM Research, Yorktown Heights, New York 10598, USA.

[12] DIFFUSE is a program that solves one- and three-dimensional forms of Fick's second equation. The code was written by G. D Alton, J. Dellwo, and I. Y. Lee.

[13] ANSYS is a finite element computer code designed to solve; the code is a

product of Swanson Analysis Systems, Inc., Houston, PA 15342-0065.

[14] FLOTRAN is a finite element code for calculating heat transfer coefficients between media interfaces; the code is a product of Swanson Analysis Systems, Inc., Houston, PA 15342-0065.

[15] G. D. Alton, D. C. Haynes, G. D. Mills, and D. K. Olsen, Nucl. Instr. and Meth., A328, (1993) 325.

[16] G. D. Alton, Particle Accelerators 47, (1994) 133.

[17] S. Sundell and H. L. Ravn, Nucl. Instr. and Meth., B70, (1992) 160.

[18] R. Kirchner, Nucl. Instr. and Meth. B70, 186 (1992).

[19] J. M. Nitschke, Nucl. Instr. and Meth. A236, (1985) 1.

[20] G. D. Alton and S. Sundell, unpublished.

[21] G. D. Alton and C. L. Williams, these proceedings.

[22] G. D. Alton and G. D. Mills, these proceedings.

[23] G. D. Alton and D. N. Smithe, Rev. Sci. Instrum. 65 (1994) 775.

[24] G. D. Alton and D. N. Smithe, Proc. of the Twelfth Int. Conf. on ECR Ion Sources, eds. M. Sekiguchi and T. Nakagawa, INS-J-182, Sept. 1995, p. 100.

[25] G. D. Alton, these proceedings.

Figure Captions

Fig. 1. ORNL-DWG 95M-9876. Vapor pressures of Al_2O_3 and AlF_3 versus temperature. Al_2O_3 is a candidate target material for production of ^{17}F and ^{18}F at the HRIBF. The radioactive ^{17}F and ^{18}F species are expected to be released from Al_2O_3 in the molecular form AlF_x.

Fig. 2. ORNL-DWG 95M-8504. TRIM simulation of a heavy ion beam at MeV energy implanted into a target material.

Fig. 3. ORNL-DWG 95M-9957. Typical "beam-on-target" and "beam-off-target" time release spectra for ^{37}Cl implanted into and released from planar/geometry CeS target. The dashed line represents a fit to the experimental data, derived by iteratively solving Fick's second equation (Eq. 3) by the use of the computer code, DIFFUSE (Ref. 12). Target temperature: 1690°C; implantation depth: 2.6 μm; diffusion coefficient: $D = 4.4 \times 10^{-10}$ cm^2/s.

Fig. 4. ORNL-DWG 95M-9655. Theoretical "beam-on-target" and "beam-off-target" time-release spectra for ^{37}Cl and ^{33}Cl diffusing from homogeneously distributed, 5-μm-diameter spherical-geometry macro-particles of CeS at 1690°C as predicted by use of the computer code DIFFUSE [12]. The code was utilized to determine the diffusion coefficient D by iteratively fitting solutions to Fick's second equation (Eq. 3) to the experimental data taken at 1690°C displayed in Fig. 3. The predictions, made for the diffusion release at a target temperature of 1990°C, were estimated by assuming an activation energy of 1.0 eV which correlates with an intrinsic diffusion coefficient, $D_o = 1.6 \times 10^{-7}$ cm^2/s. Diffusion coefficient at a target temperature of T = 1690°C: $D = 4.4 \times 10^{-10}$ cm^2/s.

Fig. 5. ORNL-DWG 95M-9695. Typical "beam-on-target" and "beam-off-target" time-release spectra for ^{78}Se implanted into and diffused from Zr_5Ge_3 planar-geometry targets. The solid line represents a fit to the experimental data derived by iteratively solving Fick's second equation (Eq. 3) by use of the computer program DIFFUSE (Ref. 12). Target temperature: 1695°C; diffusion coefficient: $D = 5.1 \times 10^{-8}$ cm^2/s.

Fig. 6. ORNL-DWG 95M-9696. Theoretical "beam-on-target" time-release spectra for homogeneously distributed ^{78}Se and ^{71}Se diffusing from 20-μm and 200-μm spherical-geometry and 20-μm and 200-μm-thick planar-geometry Zr_5Ge_3 targets as predicted by the use of the computer program DIFFUSE (Ref. 12) with S represented by a Gaussian distribution (Eq. 7). Target temperature: 1695°C; diffusion coefficient: $D = 5.1 \times 10^{-8}$ cm^2/s.

Fig. 7. ORNL-DWG 95-10132. Composite target matrixes with good diffusion release, effusive flow, and heat transport, under consideration for use at the HRIBF.

Fig. 8. ORNL-DWG 94M-8758R. Photograph of a carbon-bonded-carbon fiber (CBCF) matrix (fiber diameter $\simeq$ 6 μm) precoated with ~ 1 μm of Re followed by chemical vapor by deposition (CVD) of $\simeq$ 5 μm of SiC. The composite target matrix is highly

permeable and will be tested for the release of ^{30}S in the form of CS_2.

Fig. 9. ORNL-DWG 95-10133. Schematic drawing of a removable/insertable composite target/heat-sink system showing the components which make up the system now under design at the HRIBF for use in RIB generation. The target material may be particulate, plated onto component target support disks or fibers as illustrated in Fig. 7.

Fig. 10. ORNL-DWG 95-10134. Schematic drawing of a side view of the high temperature target/ ion source assembly mounted on the high voltage platform which is designed for use at the HRIBF (Refs. 6-8).

Fig. 11. ORNL-DWG 95-10135. Cross-sectional side view of the high-temperature electron beam plasma ion source (EBPIS) target/ion source the target heater vapor transport tube and ionization chamber of the source in use at the HRIBF (Refs. 6-8).

Fig. 12. ORNL-DWG 95-10136. Cross-sectional top view of the high-temperature electron beam plasma ion source (EBPIS) source showing the target heater vapor transport tube, and ionization chamber of the source (Refs. 6-8).

Fig. 13. ORNL-DWG 95-10137. Cross-sectioned side view of the high temperature Penning Ionization Gauge (PIG) source showing the target, vapor transport tube, and ionization chamber of the source.

Fig. 14. ORNL-DWG 95M-9705. Emittance contours for the high-temperature electron beam plasma ion source (EBPIS) displayed in Figures 11 and 12. Beam energy: 20 keV.

Fig. 15. ORNL-DWG 95M-9704. Emittance contours for the Penning Ionization Gauge (PIG) source displayed in Fig. 13. Beam energy: 20 keV.

Fig. 16. ORNL-DWG 95M-9703. Comparison of the normalized emittance ϵ_n as a function of percentage of ion beam for the EBP (Figs. 11-12) and the PIG (Fig. 13) ion sources. Beam energy: 20 keV.

Table IA. Candidate Target Materials Under Consideration for Use at the HRIBF.

Table IB. Candidate Target Materials Under Consideration for Use at the HRIBF.

Table II. Summary of Release Times τ and Estimates of Diffusion Coefficients D from HRIBF Ion Implantation Studies.

Table III. Comparison of measured and calculated electron impact ionization for several elements. Calculated values were derived by use of Eq. 13.

Table IA. CANDIDATE TARGETS FOR RIB GENERATION AT THE HRIBF

Beam	$\tau 1/2$	Reaction	Target Materials	Release Products
^{13}N	9.97 m	$^{12}C(d,n)^{13}N$	C	CN_x
^{14}O	70 s	$^{12}C(^{3}He,n)^{14}O$	C	CO
^{15}O	2.0 m	$^{12}C(^{4}He,n)^{15}O$	C	CO
^{10}C	19 s	$^{10}B(p,n)^{10}C$	BN	CN_x
^{10}C	19 s	$^{9}Be(^{3}He,2n)^{10}C$	BeO	CO
^{11}C	20 m	$^{11}B(p,n)^{11}C$	BN	CN_x
^{11}C	20 m	$^{9}Be(^{4}He,2n)^{11}C$	BeO	CO
^{17}F	64 s	$^{16}O(d,n)^{17}F$	Al_2O_3	F_x,OF_x,AlF_x
^{18}F	1.8 h	$^{17}O(d,n)^{18}F$	Al_2O_3	F_x,OF_x,AlF_x
^{17}F	6.4 s	$^{14}N(^{4}He,n)^{17}F$	BN	BF_x
^{18}F	1.8 h	$^{15}N(^{4}He,n)^{18}F$	BN	BF_x
^{21}Na	22.5 s	$^{24}Mg(p,\alpha)^{21}Na$	MgO	Na,NaO
^{29}P	4.1 s	$^{28}Si(d,n)^{29}P$	Si,SiC,SiO_2	P_xO_y
^{29}P	4.1 s	$^{27}Al(^{3}He,n)^{29}P$	AlN, AlB_2,$AlPO_4$	P_xO_y
^{30}P	2.5 m	$^{30}Si(p,n)^{30}P$	Si,SiC,SiO_2	P_xO_y
^{30}P	2.5 m	$^{27}Al(^{4}He,n)^{30}P$	AlN,AlB_2,$AlPO_4$	P_xO_y
^{30}S	1.2 s	$^{28}Si(^{3}He,n)^{30}S$	SiO_2	S,SO_x
^{30}S	1.2 s	$^{28}Si(^{4}He,2n)^{30}S$	SiO_2	S,SO_x
^{30}S	1.2 s	$^{28}Si(^{3}He,n)^{30}S$	SiC	CS_x
^{30}S	1.2 s	$^{28}Si(^{4}He,2n)^{30}S$	SiC	CS_x
^{31}S	2.9 s	$^{28}Si(^{4}He,n)^{31}S$	SiO_2	S,SO_x
^{31}S	2.9 s	$^{28}Si(^{4}He,n)^{31}S$	SiC	CS_x
^{33}Cl	2.5 s	$^{32}S(d,n)^{33}Cl$	CeS	MCl_x

Table IB. CANDIDATE TARGETS FOR RIB GENERATION AT THE HRIBF (continued)

Beam	$\tau 1/2$	Reaction	Target Materials	Release Products
^{34}Cl	32 m	$^{34}S(p,n)^{34}Cl$	CeS	MCl_x
^{36}K	0.34 s	$^{40}Ca(p,\alpha n)^{36}K$	CaO	K,KO
^{37}K	1.3 s	$^{40}Ca(p,\alpha)^{37}K$	CaO	K,KO
^{38}K	7.5 m	$^{40}Ca(d,\alpha)^{38}K$	CaO	K,KO
^{52}Fe	8.28 h	$^{52}Cr(^{3}He,3n)^{52}Fe$	C,CrAl,Cr_2O_3	Fe
^{52}Fe	8.28 h	$^{50}Cr(^{3}He,n)^{52}Fe$	C,CrAl,Cr_2O_3	Fe
^{58}Cu	3.25	$^{58}Ni(p,n)^{58}Cu$	NiAl,NiO	Cu
^{63}Ga	31 s	$^{64}Zn(p,2n)^{63}Ga$	ZnO	Ga
^{64}Ga	74 s	$^{64}Zn(p,n)^{64}Ga$	ZnO	Ga
^{63}Ga	31 s	$^{64}Zn(p,2n)^{63}Ga$	Zn_2SiO_4	Ga
^{64}Ga	74 s	$^{64}Zn(p,n)^{64}Ga$	Zn_2SiO_4	Ga
^{63}Ga	31s	$^{64}Zn(p,2n)^{63}Ga$	Zn_2TiO_4	Ga
^{64}Ga	74s	$^{64}Zn(p,N)^{64}Ga$	Zn_2TiO_4	Ga
^{63}Ga	31 s	$^{63}Cu(^{3}He,3n)^{63}Ga$	CuO	Ga
^{64}Ga	64 s	$^{63}Cu(^{3}He,2n)^{64}Ga$	CuO	Ga
^{69}As	15 m	$^{70}Ge(p,2n)^{69}As$	Zr_5Ge_3,Ge,Ge_2O_3	As,As_2O_3
^{70}As	63 m	$^{70}Ge(p,n)^{70}As$	Zr_5Ge_3,Ge,Ge_2O_3	As,As_2O_3
^{71}Se	4.7 m	$^{70}Ge(^{3}He,2n)^{71}Se$	Ge_2O_3,Ge	Se,SeO_x
^{72}Se	8.4 d	$^{70}Ge(^{4}He,2n)^{72}Se$	Ge_2O_3,Ge	Se,SeO_x
^{73}Br	3.4 m	$^{74}Se(p,2n)^{73}Br$	La_2Se_3,EuSe,ZnSe	Br_x,$LaBr_x$,$EuBr_x$,$ZnBr_x$
^{74}Br	42 m	$^{74}Se(p,n)^{74}Br$	La_2Se_3,EuSe,ZnSe	Br_x,$LaBr_x$,$EuBr_x$,$ZnBr_x$

Table II. Summary of release times $\tau 1/2$ and diffusion coeffcients D from HRIBF ion implantation studies.

Projectile	D(measured) (cm^2/s	D_e(estimated)[1] (cm^2/s)	Target[3] material	Range, <x> (μm)	τ (s)
^{35}Cl	1.2×10^{-6}	1.1×10^{-6}	Zr_5Si_3	31.3	8.8
^{37}Cl	4.9×10^{-10}	4.1×10^{-10}	CeS	2.6	164
^{75}As	5.1×10^{-8}	9.8×10^{-8}	Zr_5Ge_3	18.3	34
^{78}Se	5.1×10^{-8}	6.8×10^{-8}	Zr_5Ge_3	17.9	51
^{78}Se	–	7×10^{-8}	Zr_5Ge_3	15.0	32
^{79}Br	5.2×10^{-7}	3.6×10^{-7}	Zr_5Ge_3	15.9	7.9
^{35}Cl	–	8.1×10^{-9}	C	6.9	59
^{63}Cu	–	7.1×10^{-7}	C	7.0	0.7
^{65}Cu	–	6.5×10^{-7}	C	7.0	0.75
^{69}Ga	–	2.2×10^{-7}	C	6.8	2.1
^{75}As	–	6.6×10^{-9}	C	6.7	68
^{78}Se	–	–	C	6.0	No release
^{79}Br	–	5.4×10^{-9}	C	6.6	80
^{35}Cl	–	2.4×10^{-9}	BN	5.0	103
^{63}Cu	–	5×10^{-8}	BN	6.5	8.5
^{65}Cu	–	4.2×10^{-8}	BN	6.5	10.5
^{69}Ga	–	1.9×10^{-8}	BN	5.9	18
^{71}Ga	–	2.5×10^{-8}	BN	5.9	14
^{35}Cl	–	9.8×10^{-11}, (4.9×10^{-11})[2]	Ta	0.9	83 (166)[2]
^{63}Cu	–	1.5×10^{-10}, (7.8×10^{-11})[2]	Ta	0.7	51 (104)[2]
^{69}Ga	–	1.2×10^{-10}, (6×10^{-11})[2]	Ta	0.7	68 (136)[2]
^{75}As	–	1.9×10^{-11}, (9.6×10^{-12})[2]	Ta	0.9	420 (840)[2]
^{78}Se	–	2.2×10^{-11}, (1.1×10^{-11})[2]	Ta`	0.9	363 (726)[2]

[1] Diffusion coefficient D_e estimated from $D_e \simeq \langle x \rangle^2/\tau$.

[2] Full thickness of Ta foil: 1.8 μm; release times (parentheses) assumed to be one-half those from semi-infinite foil. Diffusion coefficients in parentheses are calculated by use of the release times in parentheses.

[3] All target temperatures during ion implantation 1650-1700°C.

Table III. Comparisons of Calculated and Experimentally Measures Ionization Efficiencies η for Electron Beam Plasma Ion Sources. Estimated ionization efficiencies were calculated by using Eq. 13.

Z	Element	I_p(eV)	N_e	η_{calc}(%)	η_{exp}(%)	Ref.
10	^{20}Ne	21.56	8	2.0	1.6	18
18	^{40}Ar	15.76	8	16.6	19	18
24	^{54}Cr	6.77	1	37.0	>20	19
26	^{57}Fe	7.90	2	45.2	30	18
32	^{76}Ge	7.90	4	65.6	41	18
36	^{84}Kr	14.00	8	34.1	35	18
36	^{84}Kr	14.00	8	34.1	36	19
46	^{100}Pd	8.33	18	89.5	>25	18
47	^{107}Ag	7.58	1	38.7	47	18
47	^{109}Ag	7.58	1	38.9	50	18
50	^{116}Sn	7.34	4	74.0	53	18
50	^{124}Sn	7.34	4	74.6	54	18
54	^{129}Xe	12.13	8	54.6	52	18
54	^{132}Xe	12.13	8	54.8	53	20
54	^{132}Xe	12.13	8	54.8	56	18
79	^{197}Au	9.23	1	32.9	50	18
83	^{209}Bi	7.29	5	82.9	68.3	18

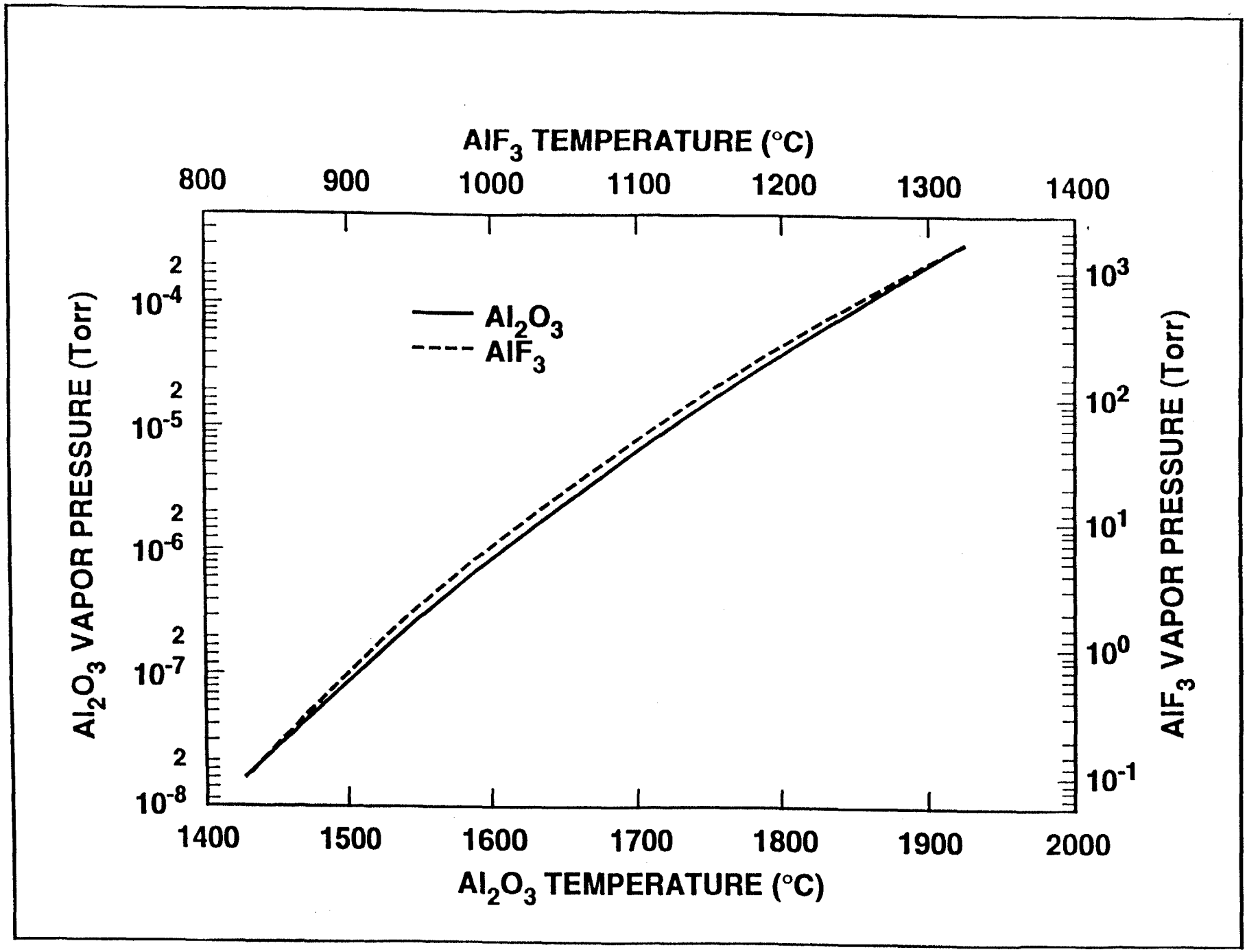
AlF3 TEMPERATURE (°C)
800
900
1000
1100
1200
1300
1400
Al2O3 VAPOR PRESSURE (Torr)
2 10-4
2 10-5
2 10-6
2 10-7
2 10-8
Al2O3
AlF3
103
102
101
100
10-1
AlF3 VAPOR PRESSURE (Torr)
1400
1500
1600
1700
1800
1900
2000
Al2O3 TEMPERATURE (°C)

Fig.1

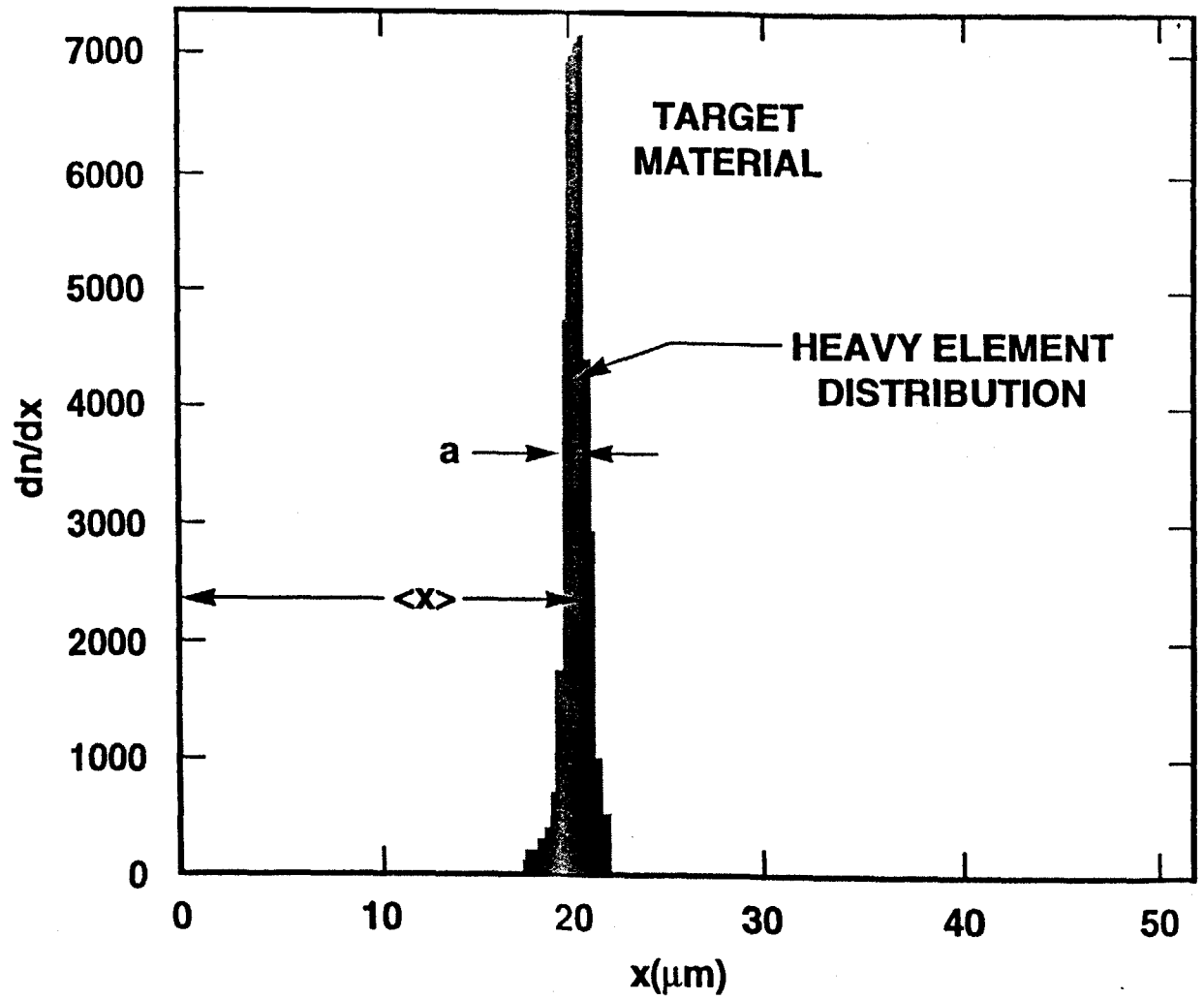
7000
6000
5000
4000
3000
2000
1000
0
dn/dx
TARGET
MATERIAL
HEAVY ELEMENT
DISTRIBUTION
a
<x>
0
10
20
30
40
50
x(μm)

Fig. 2

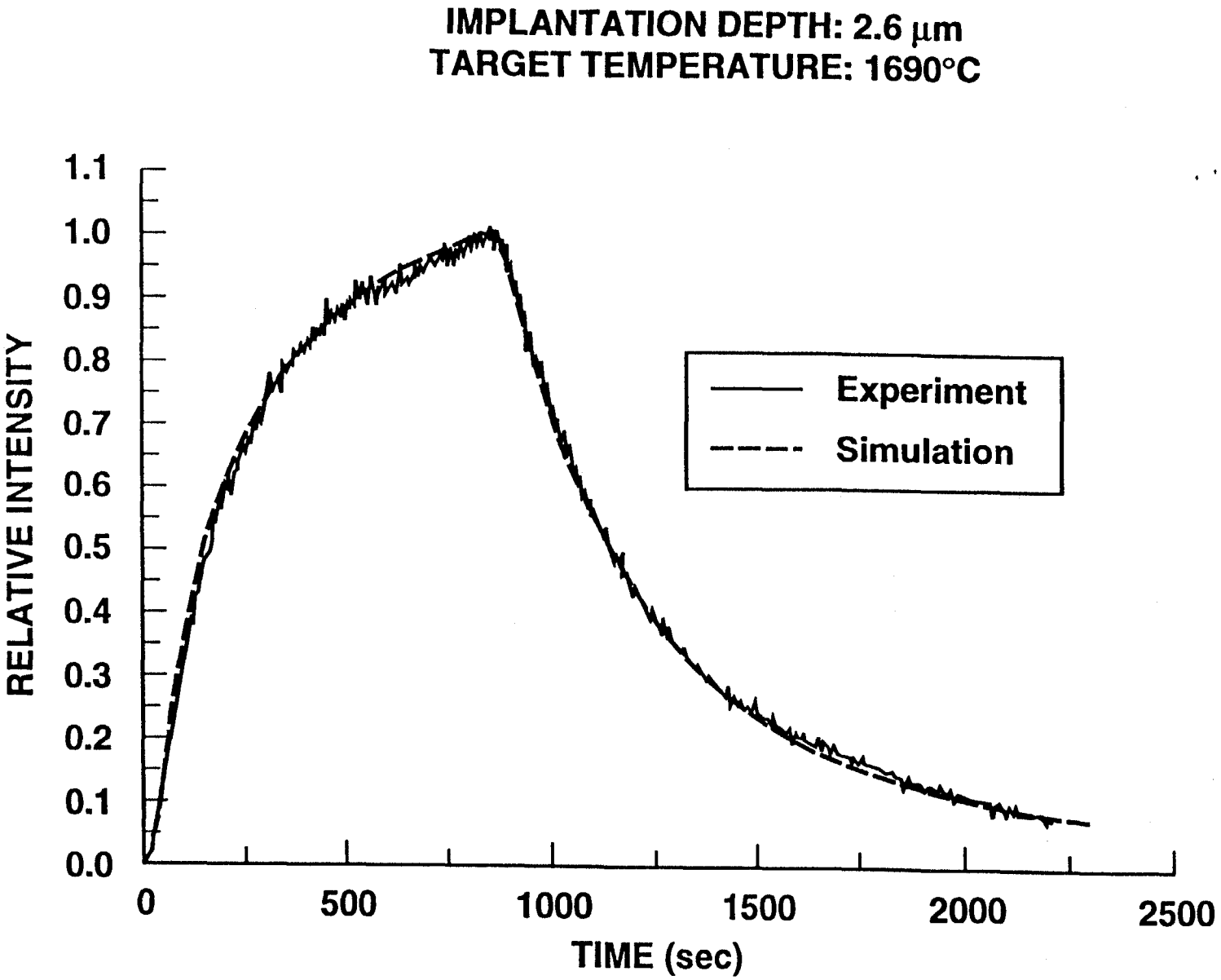
IMPLANTATION DEPTH: 2.6 μm
TARGET TEMPERATURE: 1690°C
RELATIVE INTENSITY
1.1
1.0
0.9
0.8
0.7
0.6
0.5
0.4
0.3
0.2
0.1
0.0
0
500
1000
1500
2000
2500
TIME (sec)
Experiment
Simulation

Fig. 3

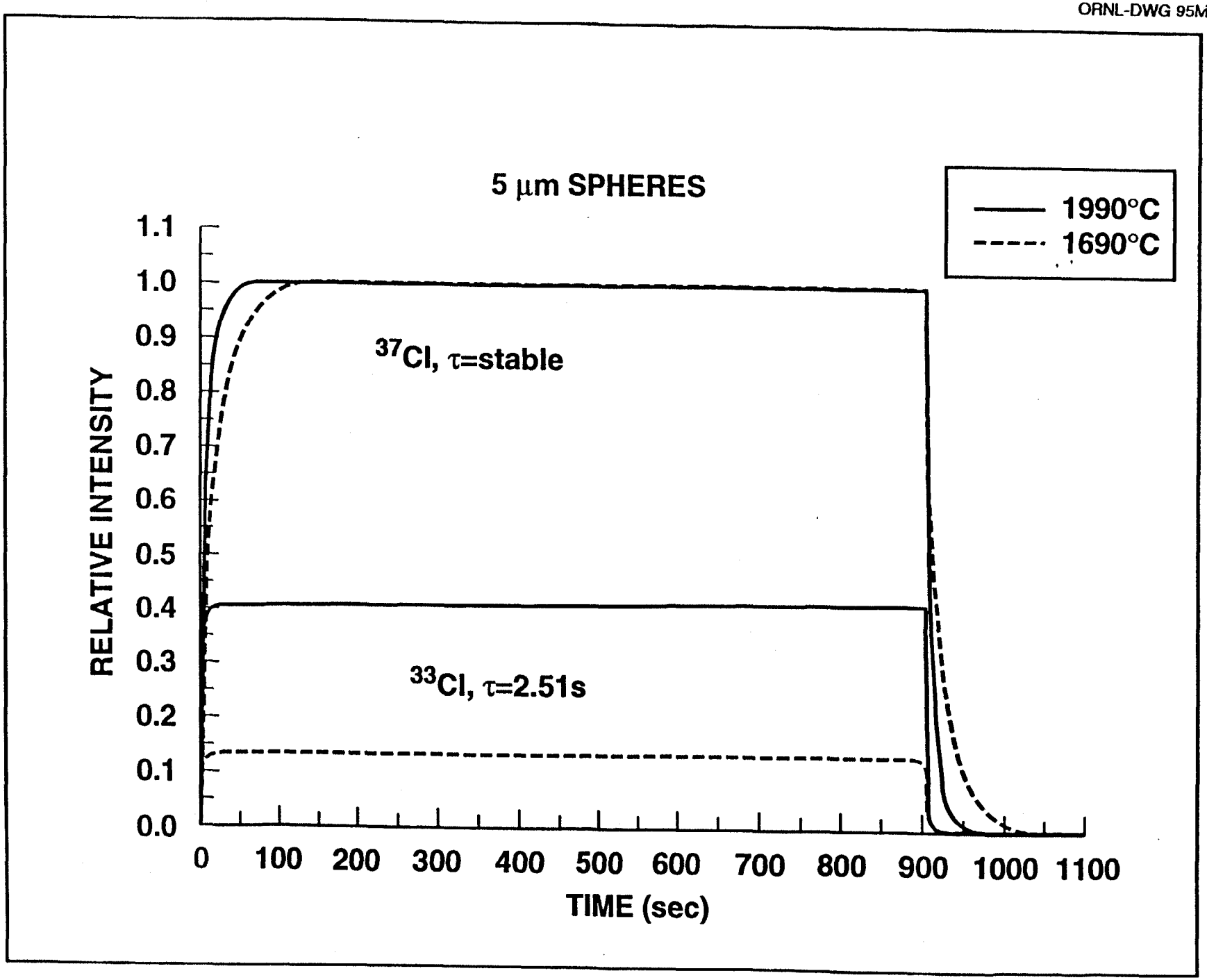
5 μm SPHERES
1990°C
1690°C
^{37}Cl, τ=stable
^{33}Cl, τ=2.51s
RELATIVE INTENSITY
1.1
1.0
0.9
0.8
0.7
0.6
0.5
0.4
0.3
0.2
0.1
0.0
0
100
200
300
400
500
600
700
800
900
1000
1100
TIME (sec)

Fig.4

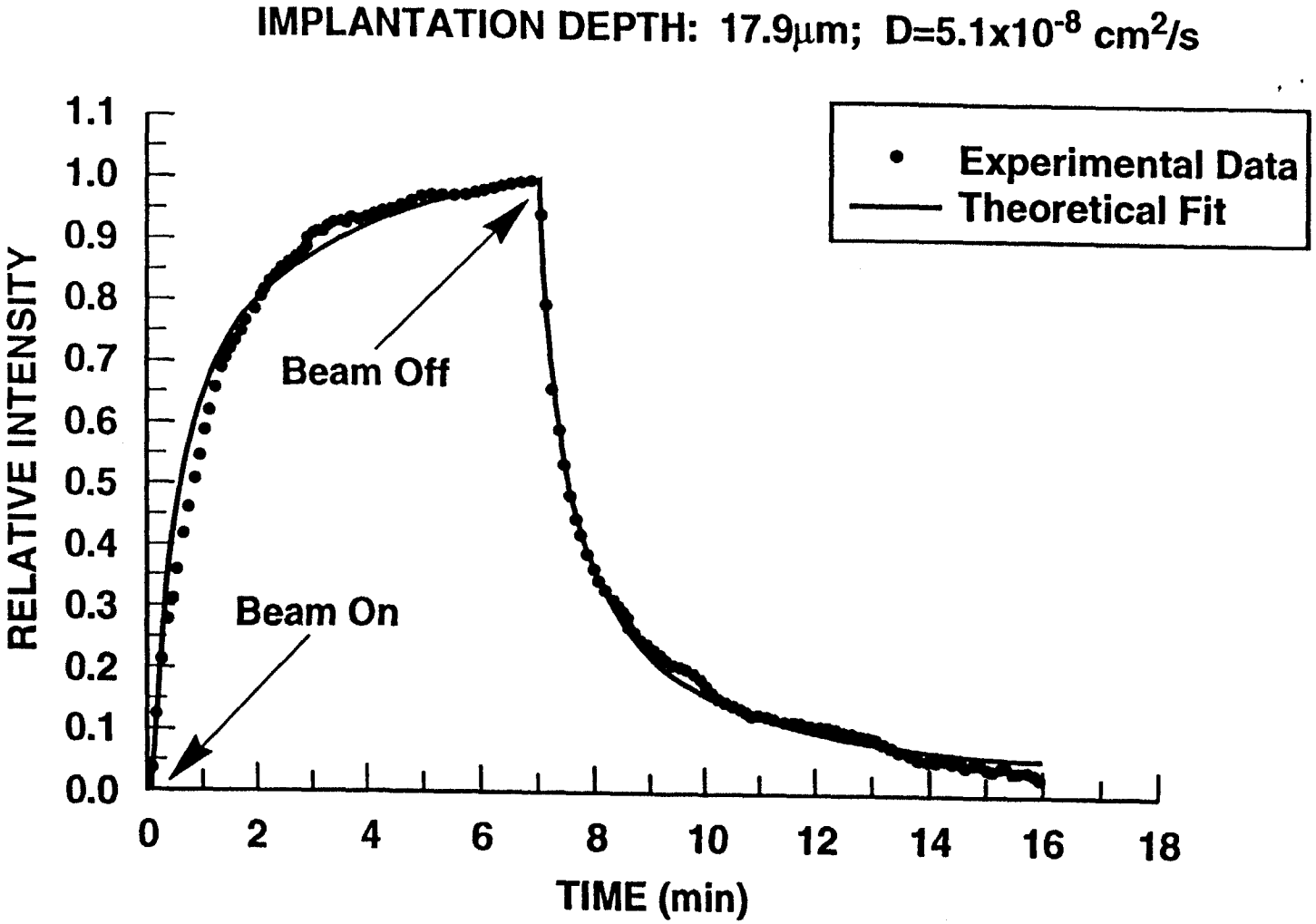
IMPLANTATION DEPTH: 17.9μm; D=5.1x10-8 cm2/s
Experimental Data
Theoretical Fit
Beam Off
Beam On
RELATIVE INTENSITY
TIME (min)
0.0
0.1
0.2
0.3
0.4
0.5
0.6
0.7
0.8
0.9
1.0
1.1
0
2
4
6
8
10
12
14
16
18

Fig. 5

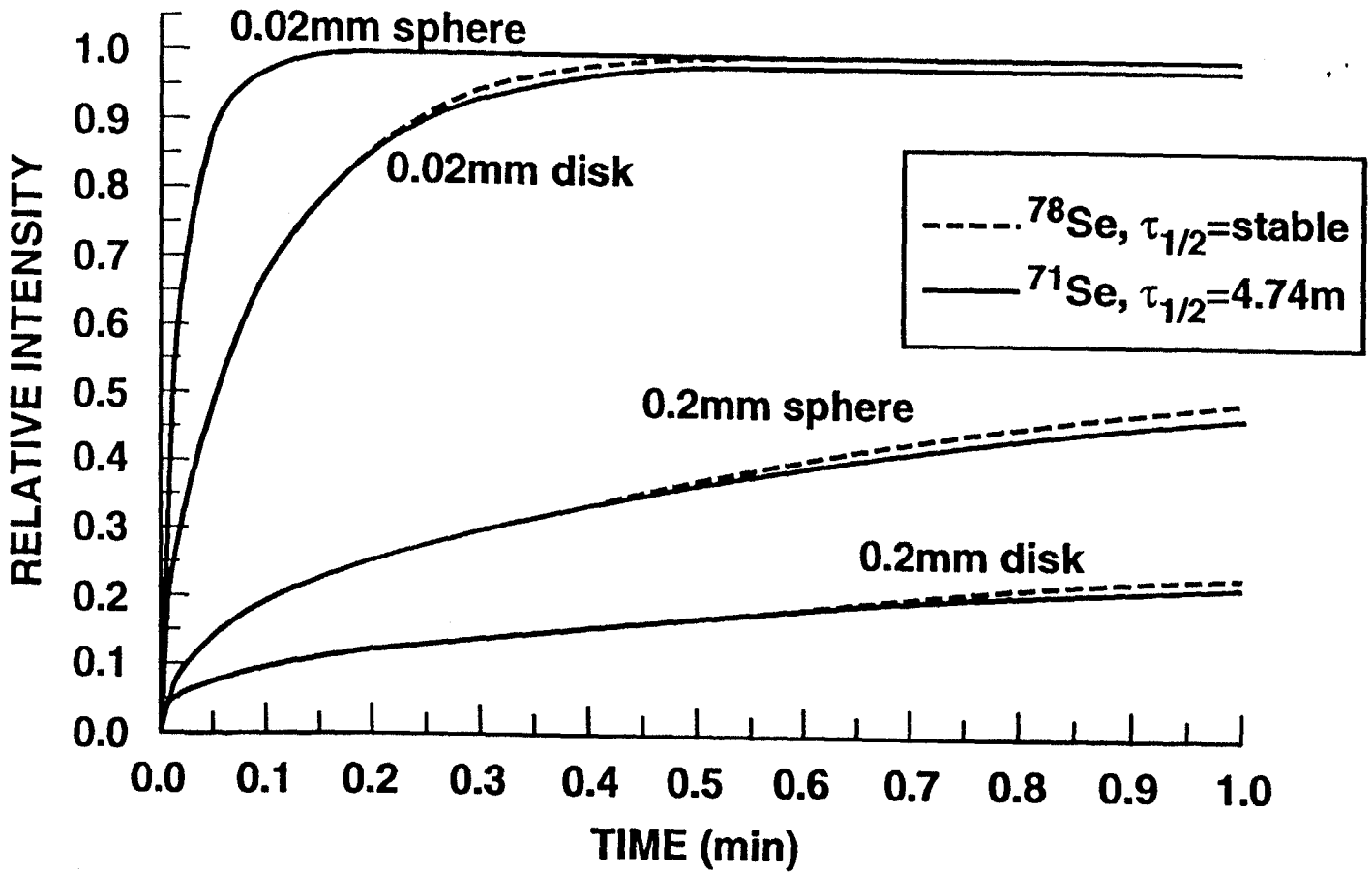
0.02mm sphere
0.02mm disk
0.2mm sphere
0.2mm disk
^{78}Se, $\tau_{1/2}$=stable
^{71}Se, $\tau_{1/2}$=4.74m
RELATIVE INTENSITY
TIME (min)
0.0
0.1
0.2
0.3
0.4
0.5
0.6
0.7
0.8
0.9
1.0

Fig. 6

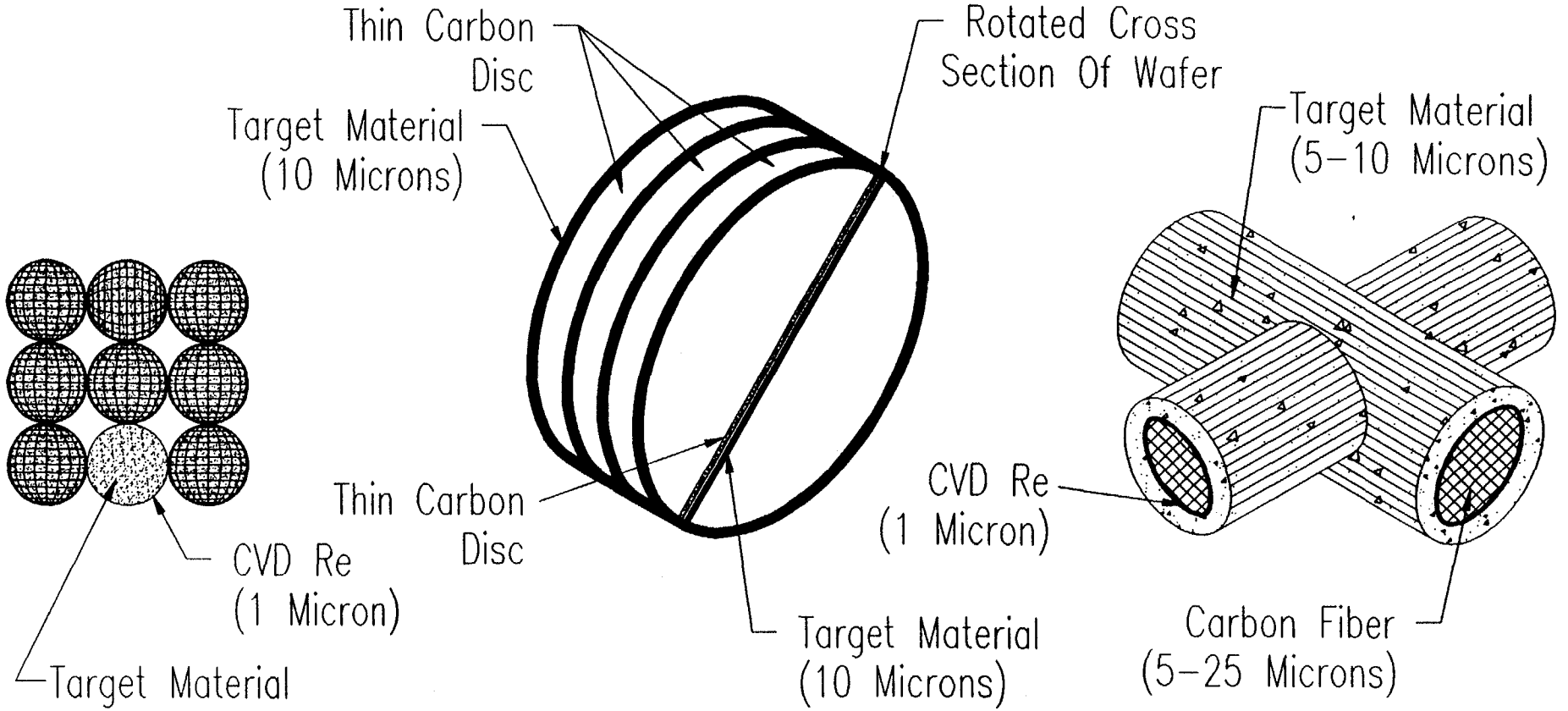

Spherical Macro-particles

Stacked Cylindrical Disks (Composite Wafers)

Reticulated Carbon/Carbon Bonded Composite Matrix

Fig. 7

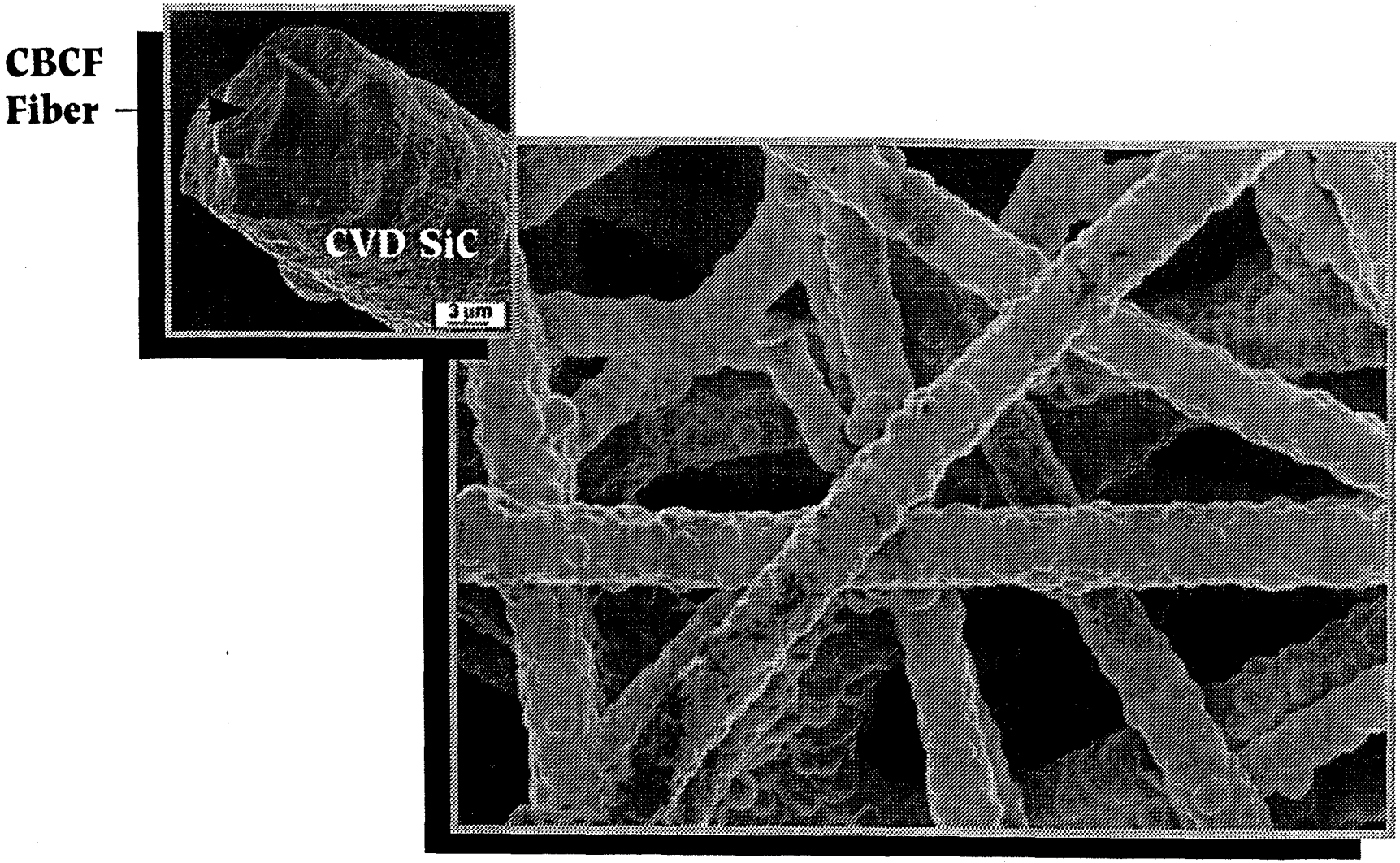

Fig. 8

ORNL-DWG 95-10133

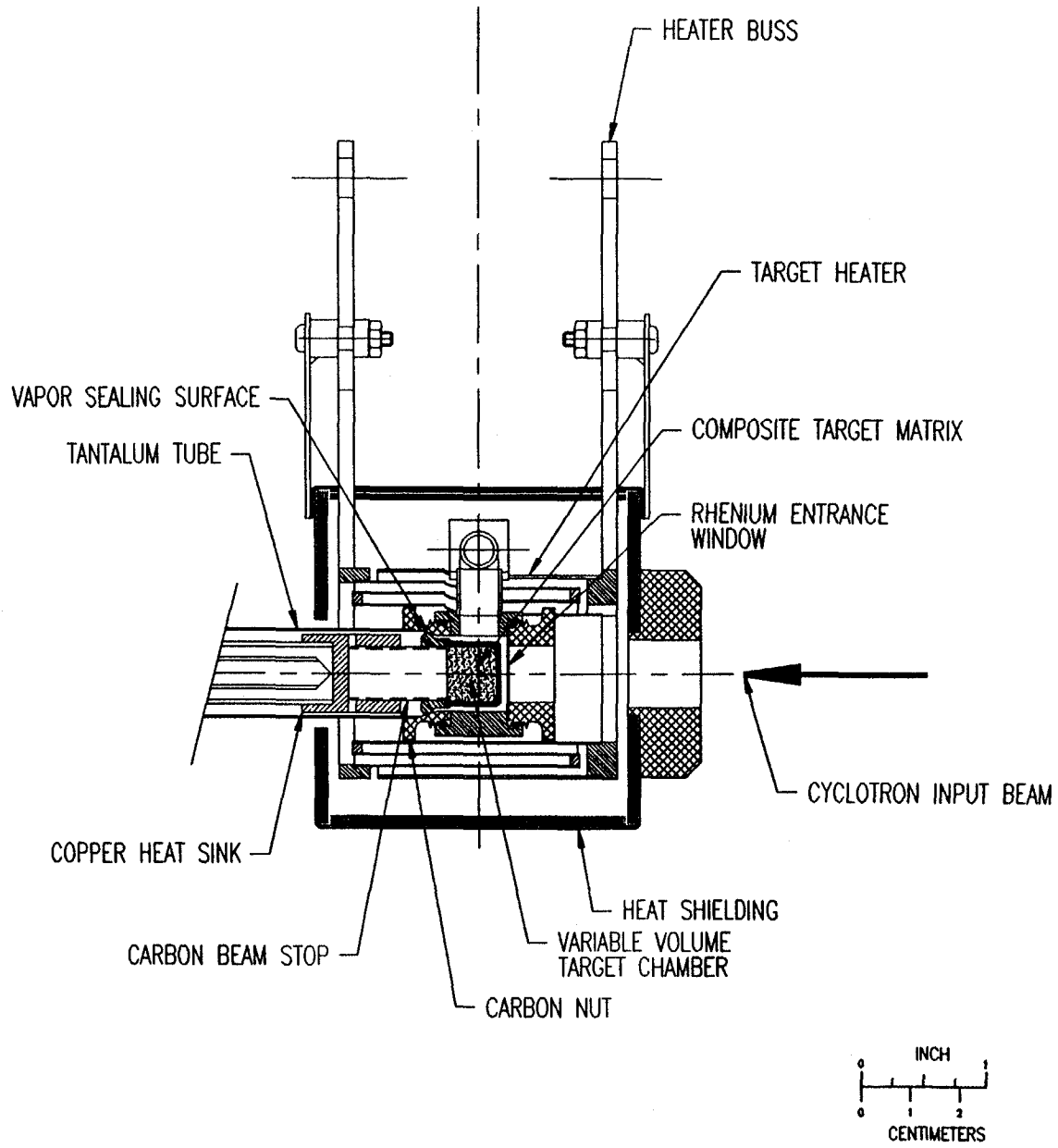

Fig. 9

ORNL-DWG 95-10133

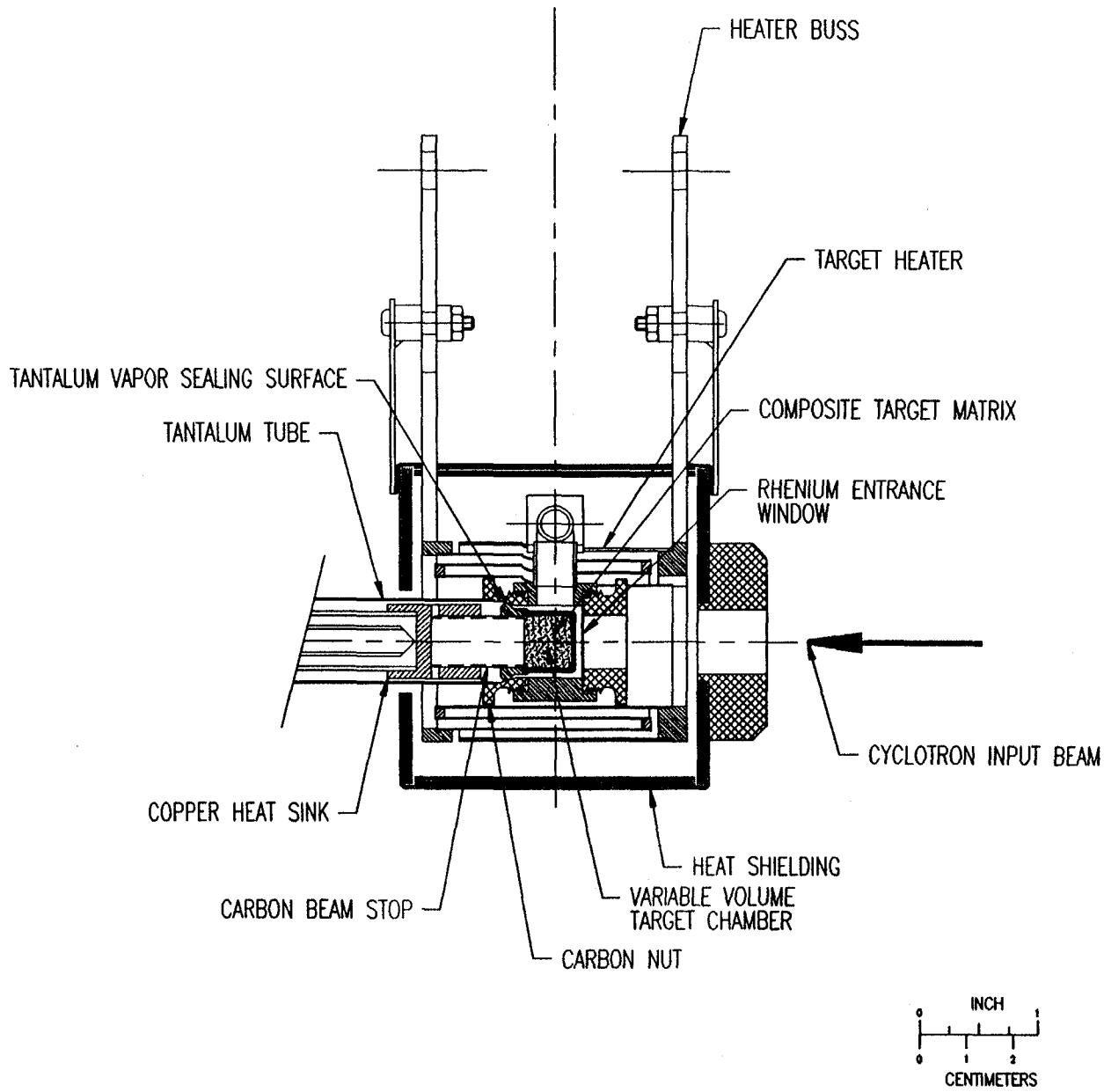

Fig. 9

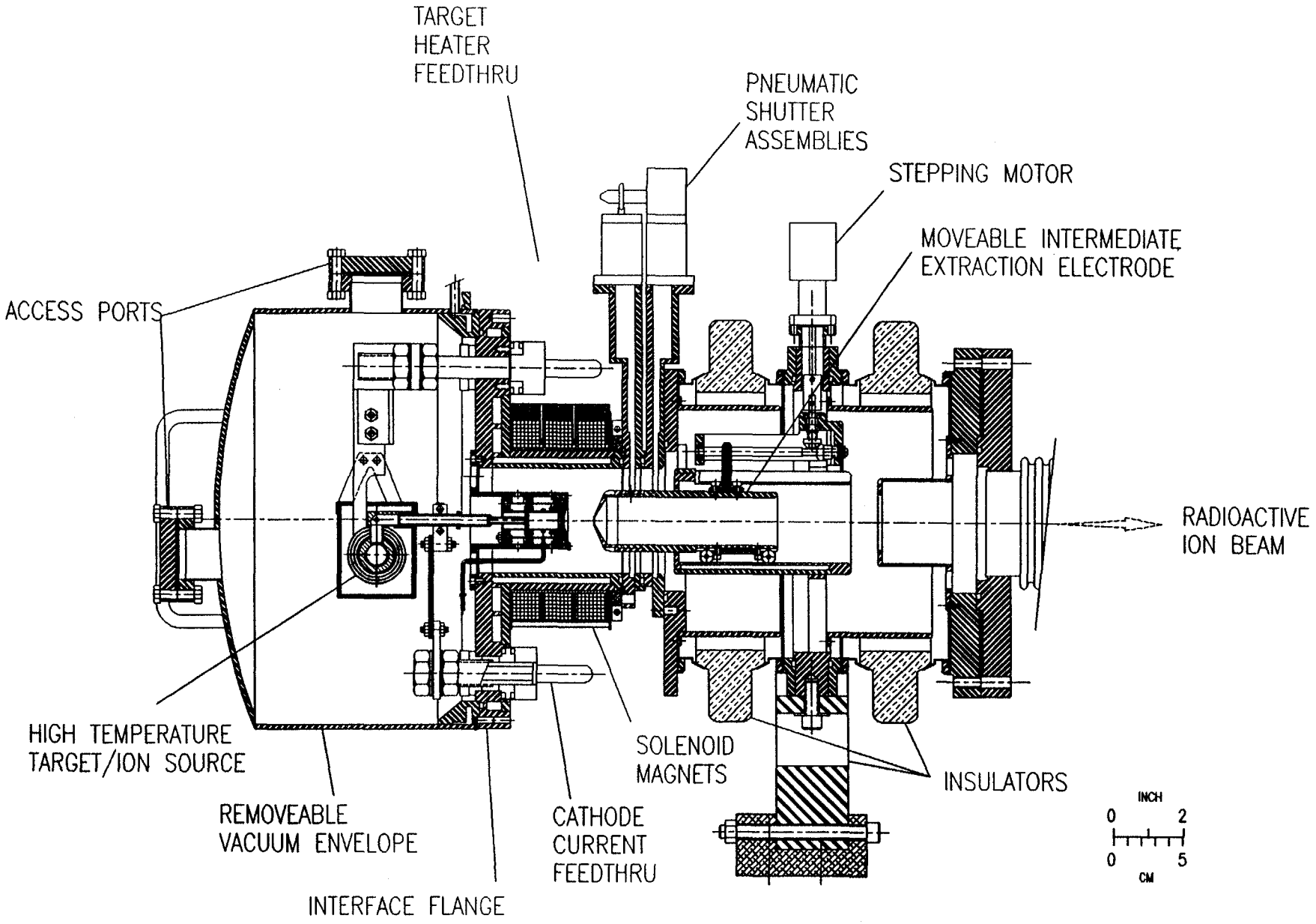
TARGET
HEATER
FEEDTHRU
PNEUMATIC
SHUTTER
ASSEMBLIES
STEPPING MOTOR
MOVEABLE INTERMEDIATE
EXTRACTION ELECTRODE
ACCESS PORTS
RADIOACTIVE
ION BEAM
HIGH TEMPERATURE
TARGET/ION SOURCE
SOLENOID
MAGNETS
INSULATORS
REMOVEABLE
VACUUM ENVELOPE
CATHODE
CURRENT
FEEDTHRU
INTERFACE FLANGE
INCH
0 2
0 5
CM

Fig.10

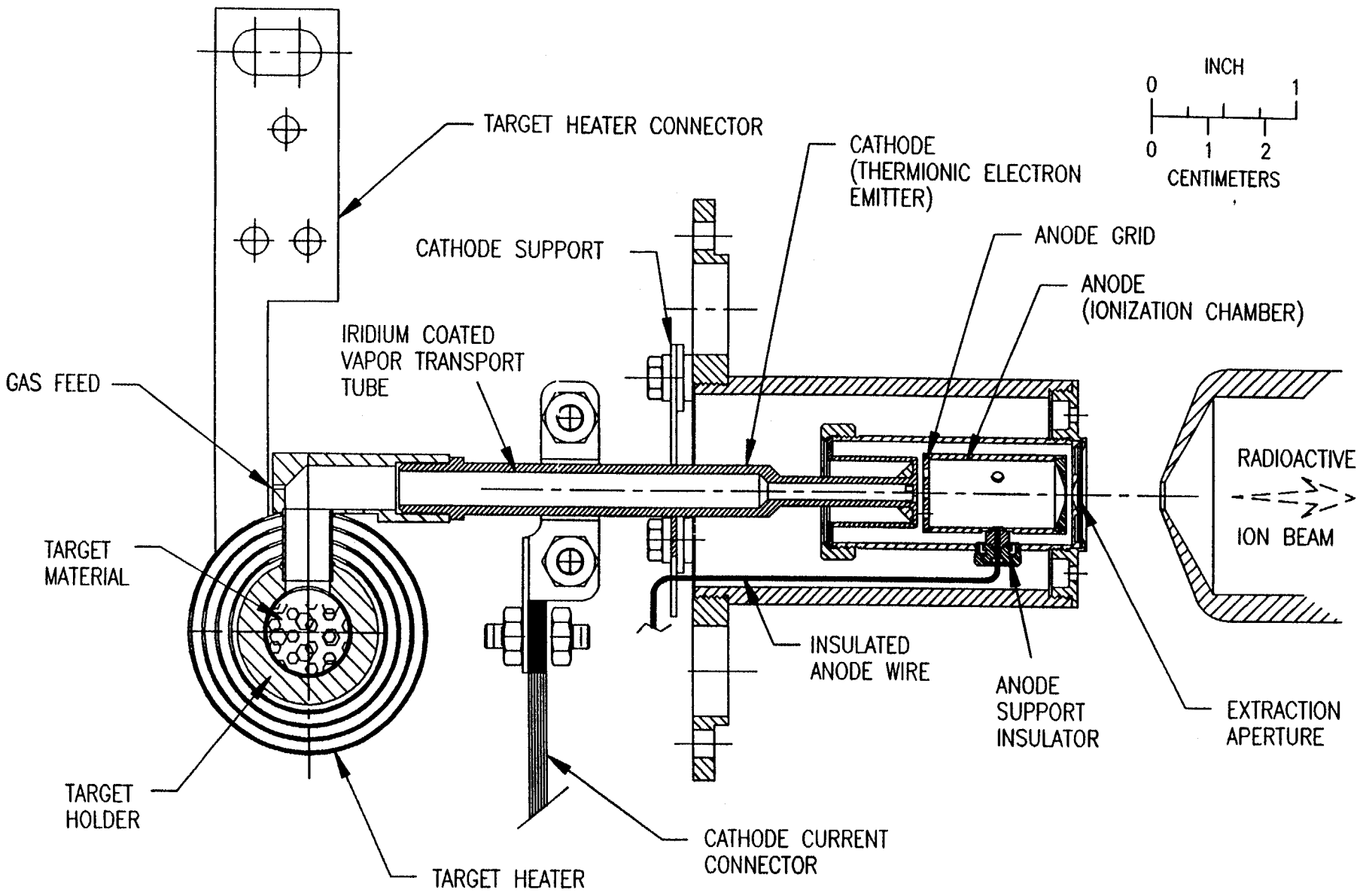

SIDE VIEW

Fig. 11

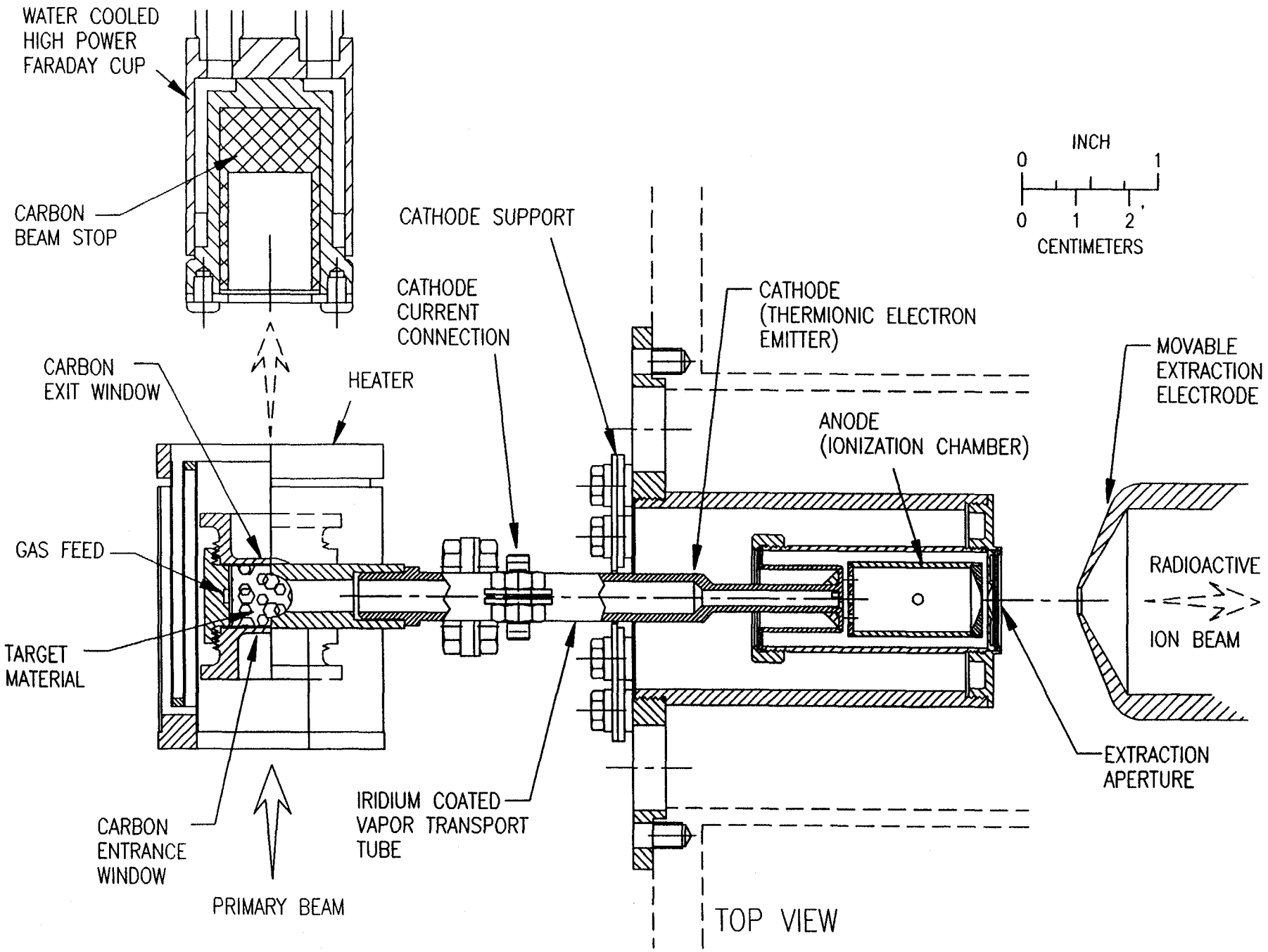
WATER COOLED
HIGH POWER
FARADAY CUP
CARBON
BEAM STOP
INCH
0 1
0 1 2
CENTIMETERS
CATHODE SUPPORT
CATHODE
CURRENT
CONNECTION
CATHODE
(THERMIONIC ELECTRON
EMITTER)
MOVABLE
EXTRACTION
ELECTRODE
CARBON
EXIT WINDOW
HEATER
ANODE
(IONIZATION CHAMBER)
GAS FEED
RADIOACTIVE
ION BEAM
TARGET
MATERIAL
EXTRACTION
APERTURE
CARBON
ENTRANCE
WINDOW
IRIDIUM COATED
VAPOR TRANSPORT
TUBE
PRIMARY BEAM
TOP VIEW

Fig. 12

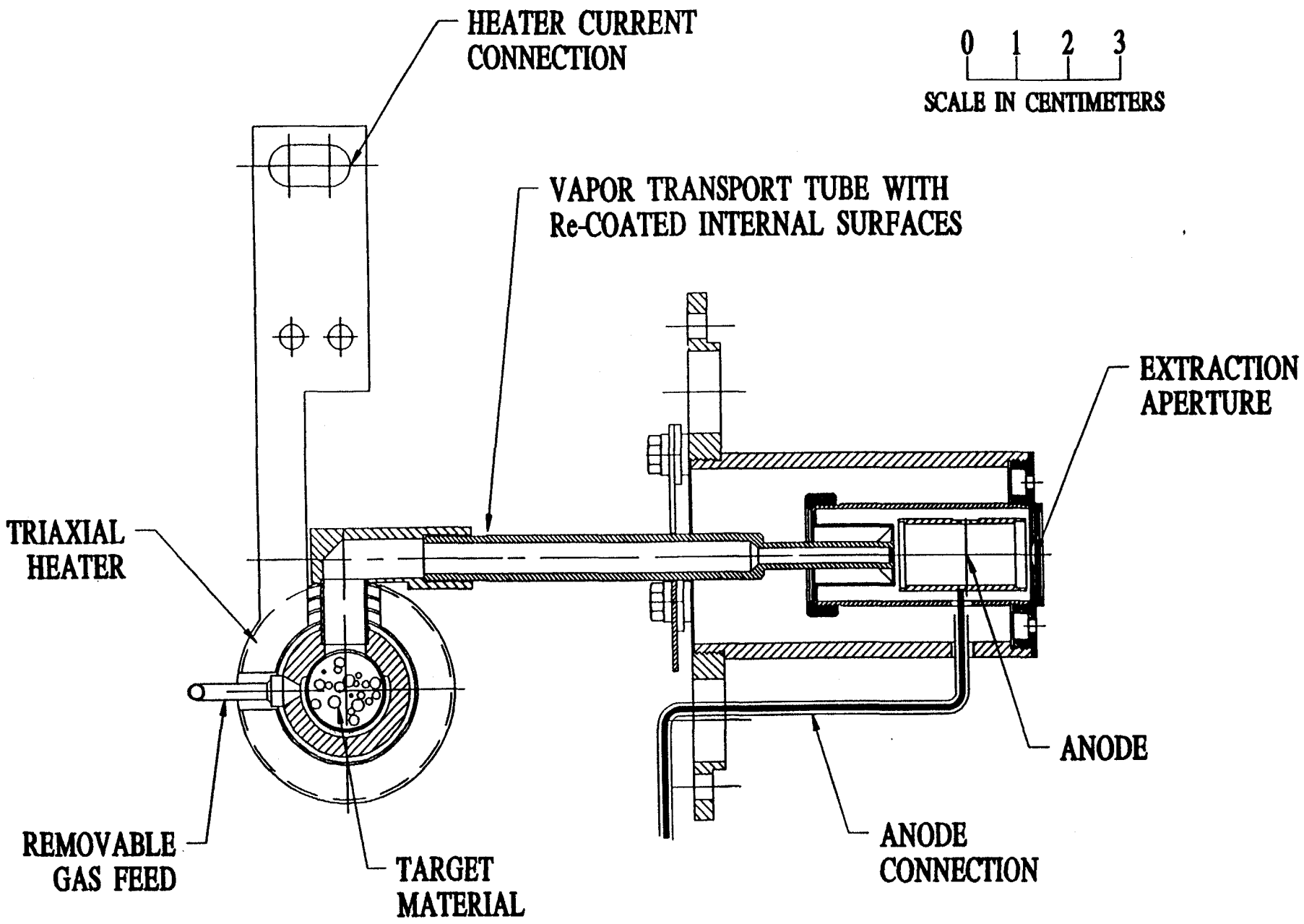
HEATER CURRENT CONNECTION
0 1 2 3
SCALE IN CENTIMETERS
VAPOR TRANSPORT TUBE WITH Re-COATED INTERNAL SURFACES
EXTRACTION APERTURE
TRIAXIAL HEATER
ANODE
REMOVABLE GAS FEED
TARGET MATERIAL
ANODE CONNECTION

Fig. 13

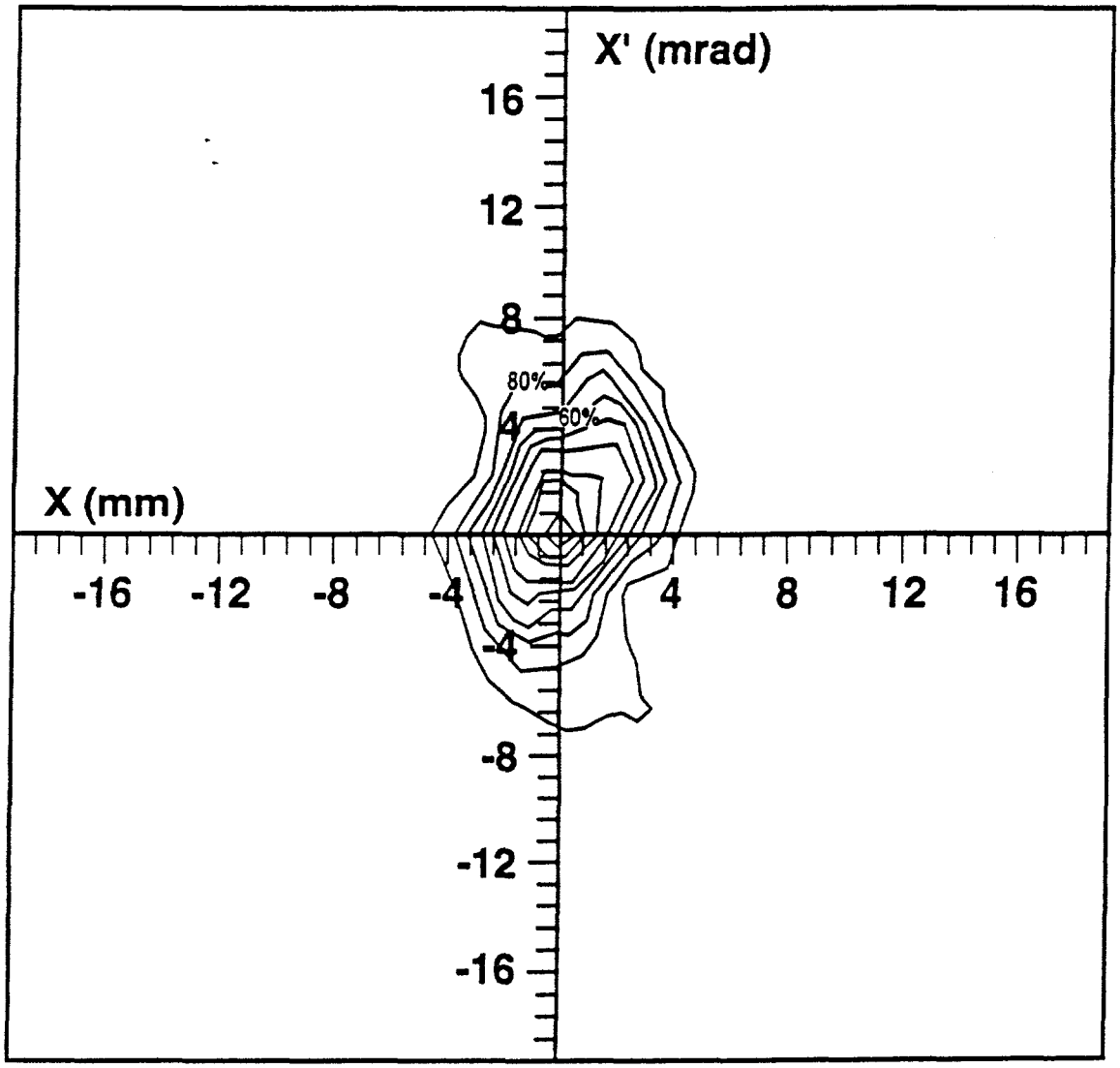

Species: Xenon	Percentage of total beam intensity	Emittance (π.mm.mrad)
Ion energy: 20 keV	10	.19
	20	1.41
Ion Source: EBPIS	30	2.42
	40	5.4
	50	7.71
	60	10.54
	70	14.11
	80	19.12
	90	31.94

Fig. 14

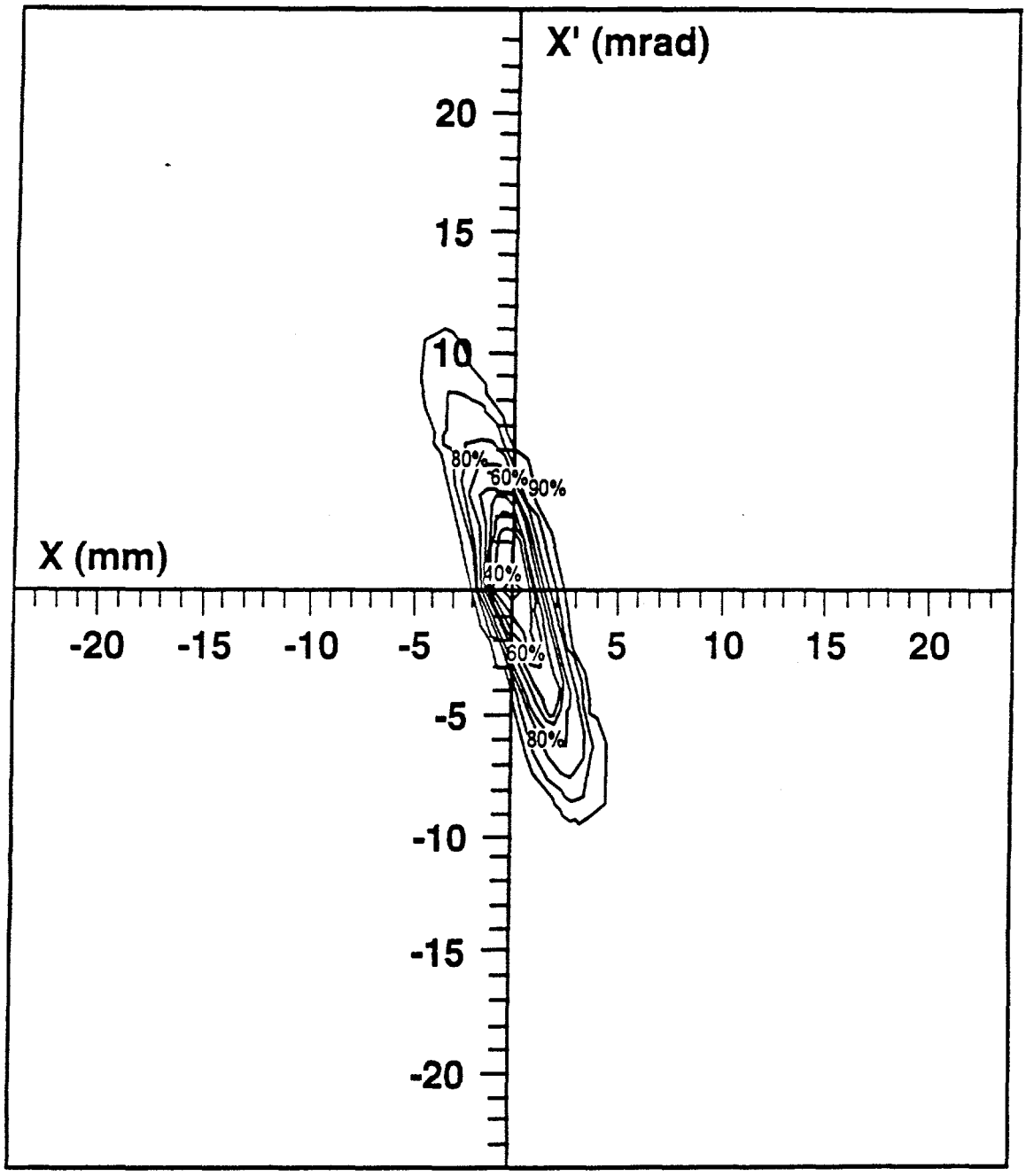

Species: Xenon

Ion energy: 20 keV

Percentage of total beam intensity	Emittance (π.mm.mrad)
10	.07
20	1.38
30	2.59
40	4.58
50	5.53
60	8.11
70	11.77
80	16.67
90	23.44

Fig. 15

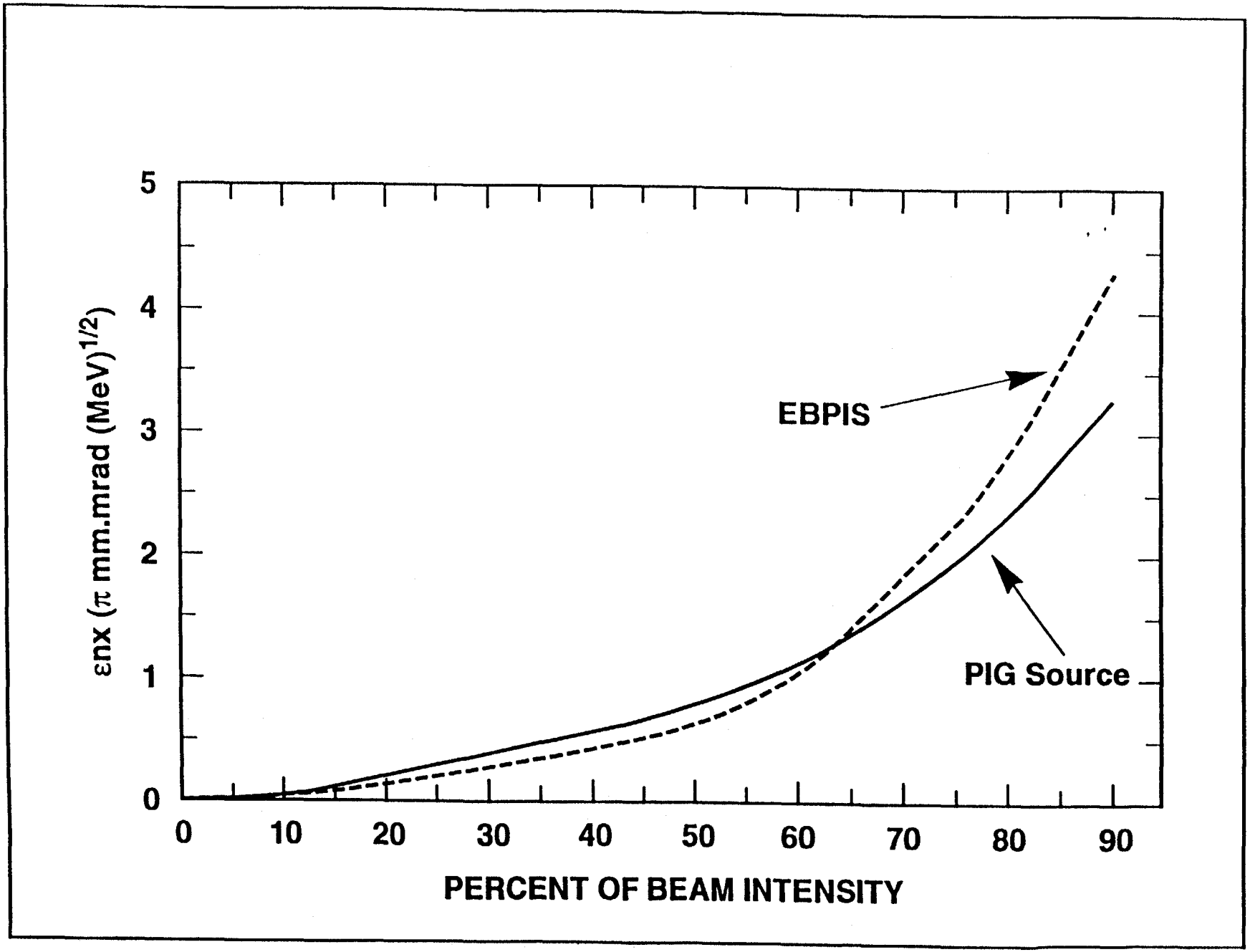
5
4
3
2
1
0
εnx (π mm.mrad (MeV)^1/2)
EBPIS
PIG Source
0
10
20
30
40
50
60
70
80
90
PERCENT OF BEAM INTENSITY

Fig.16